SLAC TRANS 41

Elektron-Photon-Kaskaden in Blei für Primärteilchen der Energie 6 Gev (Electron and photon cascades in lead due to 6 Gev primaries) by U. Völkel. [Deutsches Elektronen-Synchrotron ('DESY') (German Electron Synchrotron)] in Hamburg. Report DESY 65/6 (July 1965) 'Theorie'. Translated from the German (March 1966) by Z.F. St-Gallay.

TRANSLATED FOR
STANFORD LINEAR ACCELERATOR CENTER

****

ELECTRON AND PHOTON CASCADES IN LEAD DUE TO 6 Gev PRIMARIES

by U. Völkel

A Monte Carlo method was used to calculate the spectra of the angular and the radial distribution of the particles in electron and photon cascades due to 6 Gev primaries in lead. The energy distribution in the material was also calculated. On the basis of the similarities between these results and those obtained by Nagel[3] with less energetic incident electrons (100 to 1000 Mev), the normalized energy spectra and the angular distribution (with reservations) are seen to be independent of the incident energy up to 6 Gev.

I. Introduction

Nagel[1-3] has used the Monte Carlo method to calculate the parameters of electron and photon cascades produced in lead by particles

with incident energies up to 1000 Mev. Similar calculations have now been made for 6 Gev particles. The following cascade processes were considered in both investigations:

1) Electron bremsstrahlung

2) Moller scattering* of electrons with energy transfer $> 2\ mc^2$

---

* Translator's note: Term unfamiliar

---

3) Multiple scattering of electron

4) Energy loss of electrons due to ionization with energy transfer $< 2\ mc^2$ and to weak bremsstrahlung quanta with $k < 1/2\ mc^2$

5) Photon pair formation

6) Compton scattering of photons

7) Photo-effect of the lead atom.

The reader interested in these aspects is referred to ref. 2. It should be added that by electrons we also mean positrons, which can be treated in the same manner. The electrons and the photons were monitored up to a cut-off energy of 1.5 and 0.25 Mev, respectively.

The calculations here are based on the statistical data for 200 electron cascades and 100 photon cascades. These statistics are sufficiently

representative in the case of high energies, since the results obtained from data for 100 electron cascades differ little from those obtained from the total of 200 electron cascades.

We shall deal in Sections II to VI below only with a cascade caused by primary electrons, since the relevant results can then be compared with Nagel's values. A cascade due to 6 Gev photons will be compared in Section VIIIwith that due to 6 Gev electrons. Energy is expressed in Mev, lengths in Pb-radiation length X_o ($1\ X_o = 5.84\ g/cm^2 = 0.515$ cm).

II. Cascade formation and the number of particles

To describe the cascade, let the z-axis be parallel to the axis of the cascade (plane of incidence : $z = 0$), which is also a symmetry axis. Let $\pi(E_0; E, t, r, \Theta).2r.dr.d(\cos\Theta)dE$ denote the number of electrons with incident energy of E_0 which penetrate the plane $z = t.X_0$ with an energy between E_0 and $E_0 + dE$, the distance from the cascade axis being between r and $r + dr$; the z-component of the impulse direction being between $\cos\Theta$ and $\cos\Theta + d(\cos\Theta)$. Further, let $\gamma(E_0; E,t,r,\Theta)\cdot .2\pi dr.d(\cos\Theta)dE$ denote the corresponding number of photons. By the

appropriate integration of these two functions, we can obtain all the required distributions. Thus, the integral

$$\Pi(E_0; E, t) = \int_E^{E_0} dE \int_0^1 d(\cos\vartheta) \int_0^\infty 2\pi r\, dr\, \bar{n}(E_0; E, t, r, \vartheta)$$

gives the number of electrons with energy > E, that penetrate the plane $z = t.X_0$ with an incident energy of E_0 in the 'forward' direction ($\cos\Theta > 0$). The corresponding integral for photons is $\Gamma(E_0; E, t)$. The curves obtained by plotting these two functions against t for $E_0 = 6$ Gev are shown in Figures 1 and 2, giving an indication of the cascade formation,

Nagel's[3] interpolation formulas obtained from his results for $E_0 = 100$, 200, 400, and 1000 Mev permit the calculation of the position and the height of the maxima of these curves from the incident energy E_0 and the cut-off energy E; the error is about 10%. These calculations give values of the correct order of magnitude even for $E_0 = 6$ Gev, which is much higher than the energies so far considered. The error here is 10 to 15%. The formulas given by Nagel are as follows:

$$\Pi_{max}(E_0, E) = 0{,}091 \frac{E_0 + 37{,}5}{E + 12{,}8} + 0{,}45 \quad \text{for} \quad \begin{cases} 100 \leq E_0 \leq 1000 \\ 1{,}5 \leq E \leq 20 \end{cases} \qquad (1a)$$

$$\Pi_{max}\,(E_o,\,E) = a(E)\,[E_o + 37{,}5] + 0{,}45 \quad \text{for} \begin{cases} 100 \leq E_o \leq 1000 \\ 20 \leq E \leq 50, \end{cases} \tag{1b}$$

For the position of the maximum:

$$t_{max(\pi)}\,(E_o,\,E) = 1{,}11\ \ln E_o - 0{,}25\ \ln E - 3{,}87 \quad \text{for} \begin{cases} 100 \leq E_o \leq 1000 \\ 1{,}5 \leq E \leq 15 \end{cases} \tag{2a}$$

$$t_{max(\pi)}\,(E_o,\,E) = 1{,}11 \ln E_o + b(E) \qquad \text{for} \begin{cases} 100 \leq E_o \leq 1000 \\ 15 \leq E \leq 50 \end{cases} \tag{2b}$$

Nagel[3] has also plotted the functions $a(E)$ and $b(E)$.

We have collated in Table 1 the values for $\bar{\pi}_{max}(E_o,\,E)$ and $t_{max(\bar{\pi})}(E_o, E)$ for $E_o = 6$ Gev, as calculated by our Monte Carlo method and from relations 1 and 2. The latter gave excessively high values for the number of particles and for the maxima at $E_o = 6$ Gev. In fact, the particle numbers would be better described by a somewhat modified relationship for $\bar{\pi}_{max}$ (see column 4 in Table I):

$$\Pi_{max}\,(E_o,\,E) = 0{,}08\,\frac{E_o + 37{,}5}{E + 12{,}8} + 0{,}45 \quad \text{for} \begin{cases} E_o = 6 \text{ GeV} \\ 1{,}5 \leq E \leq 1000 \end{cases} \tag{1'}$$

The maximum depth at $E_o = 6$ Gev and $E \geq 20$ Mev is very well described by the expression:

$$t_{max(\pi)}(E_o,\,E) = \ln \frac{E_o}{3\,E}, \tag{2'}$$

This expression is given by the analytical theory of cascades[4] (approximation

A) (see column 7 in Table I).

Table II contains the corresponding values for the height and the position of the maxima for the photon numbers, as calculated by the Monte Carlo method and from the following relationships[3]:

$$\Gamma_{max}\,(E_o,\,E) = 0{,}1\,\frac{E_o + 37{,}5}{E + 1{,}33} + 0{,}45 \text{ for } 0{,}25 \leq E \leq 0{,}05\,E_o \quad (= 300) \tag{3}$$

$$t_{max(\gamma)}\,(E_o,\,E) = 0{,}73\left(\frac{E_o}{E}\right)^{0{,}38} \text{ for } 10 \leq E \leq 0{,}5\,E_o \quad (= 3000) \tag{4}$$

(See Table II)

As in the case of the number of electrons, Nagel's equations again lead to excessively high values (with an error of up to 20%). The following modified equations, however, give a very good description of the Monte Carlo results (see Table II, columns 4 and 7, respectively):

$$\Gamma_{max}\,(E_o,\,E) = 0{,}09\,\frac{E_o + 37{,}5}{E + 1{,}33} + 0{,}45 \text{ for } E_o = 6 \text{ GeV}, \quad 0{,}25 \leq E \leq 600 \text{ MeV} \tag{3'}$$

$$t_{max(\gamma)}\,(E_o,\,E) = \ln\frac{E_o}{1{,}5 \cdot E} \text{ for } E_o = 6 \text{ GeV}, \; 1{,}5 \leq E \leq 80 \text{ MeV} \tag{4'}$$

Further, in agreement with the analytical theory of cascades (approximation A) the maximum number of photons depends only on E_o/E for $100 \leq E_o \leq$ 6000 Mev

and $E_0/E \leq 30$. Moreover, when $1000 \leq E_0 \leq 6000$ Mev, this relationship holds even for the case $E \geq E_0/150$ (see Figure 3).

For the sake of comparison, Figures 1 and 2 contain an exponential decrease with $e^{-\lambda_{min} t}$, where λ_{min} is the minimum photon absorption coefficient in lead ($\lambda_{min} = 0.24\ X_0^{-1}$). On the basis of qualitative considerations, the curves for the number of particles should exhibit approximately the same decrease in the case of large values of t.

III. R a d i a l d i s t r i b u t i o n

The radial distribution at depth t is given by

$$\pi(E_0; t, r) = \int_{1,5}^{E_0} dE \int_0^1 d(\cos\vartheta)\ \pi(E_0; E, t, r, \vartheta)$$

for electrons, and by

$$\gamma(E_0; t, r) = \int_{0,25}^{E_0} dE \int_0^1 d(\cos\vartheta)\ \gamma(E_0; E, t, r, \vartheta)$$

for photons.

The expression $\pi(E_0,t,r).2rdr$ denotes the number of electrons penetrating the plane $z = t.X_0$ in the 'forward' direction ($\cos\Theta > 0$); they are at a distance between r and $r + dr$ from the cascade axis. The corresponding expression for photons is $\gamma(E_0,t,r).2rdr$. Figures 4,

5a, and 5b show the radial distribution at various depths t, clearly indicating the gradual lateral widening of the cascades.

IV. Spectra and angular distribution

Nagel has verified the following rules for the electron spectra: 'When the depth is measured in units of the maximum thickness $t_{max(\pi)}(E_0, mc^2)$, the form of the electron spectrum is, in a first approximation, independent of the incident energy E_0'. The same applies to the photon spectra and to the angular distributions of both types of particle, if the unit of length is the maximum penetration thickness of the electrons $t_{max(\pi)}(E_0, mc^2)$. When E_0 = 6 Gev, the following value is obtained for $t_{max(\pi)}$ by extrapolation:

$$t_{max(\pi)}\ (6\ \text{GeV},\ mc^2) \approx 6\ X_0.$$

From the electron spectrum

$$\pi(E_0; E, t) = \int_0^1 \alpha(\cos\vartheta) \int_0^\infty 2\pi r\, dr\ \pi(E_0; E, t, r, \vartheta)$$

and the photon spectrum

$$\gamma(E_0; E, t) = \int_0^1 \alpha(\cos\vartheta) \int_0^\infty 2\pi r\, dr\ \gamma(E_0; E, t, r, \vartheta)$$

we obtain the relative energy distributions by normalization of the particles in the forward direction:

$$\omega_e(E_0; E, t) = \pi(E_0; E, t) / \Pi(E_0, 15, t)$$

$$\omega_\gamma(E_0; E, t) = \gamma(E_0; E, t) / \Gamma(E_0, 925, t)$$

The curves obtained by plotting $\omega_e(E_0; E, \tau)$ and $\omega_\gamma(E_0; E, \tau)$ against E at a fixed value of $\tau = t_{max(\pi)}(E_0, mc^2)$ should therefore be independent of E_0. Figures 6a-d and 7a-c show that this also applies for $E_0 = 6$ Gev. In each case, the actual curve shows the energy distribution found by Nagel for $100 \leq E_0 \leq 1000$. For the sake of comparison with Nagel's values for 1 Gev, our calculated values at $E_0 = 6$ Gev are shown in circles.

Figures 8, 9a and 9b show the spectra of $\pi(E_0, E, t)$ and $\gamma(E_0, E, t)$ for $E_0 = 6$ Gev and several values of the depth t. Even for larger values of t the maximum of the photon spectra lies at about 1 to 1.2 Mev, not at the energy with the smallest absorption coefficient λ_{min} (i.e. at about 3 to 4 Mev) as given by qualitative considerations.

To obtain the angular distribution at depth t, we assume that the probability for a particle with direction $\cos\Theta$ to penetrate the plane $z = t.X_0$ is proportional to $|\cos\Theta|$. We therefore construct the integrals:

$$\pi(E_0; t, \vartheta) = \frac{1}{|\cos\vartheta|} \int_{1,5}^{E_0} dE \int_0^{\infty} 2\pi\, dr\ \pi(E_0; E, t, r, \vartheta)$$

$$\gamma(E_0; t, \vartheta) = \frac{1}{|\cos\vartheta|} \int_{0,25}^{E_0} dE \int_0^{\infty} 2\pi\, dr\ \gamma(E_0; E, t, r, \vartheta)$$

The relative angular distributions

$$w_e(E_0; \tau, \vartheta) = \pi(E_0; \tau, \vartheta) \,/\, \Pi(E_0, 1,5, \tau)$$

$$w_\gamma(E_0; \tau, \vartheta) = \gamma(E_0; \tau, \vartheta) \,/\, \Gamma(E_0; 0,25, \tau)$$

should be independent of E_0 for a fixed value of $\tau = \lambda t_{max(\pi)}(E_0, mc^2)$. In this case, however, the plots for E_0 = 6 Gev systematically lie above Nagel's curves (see Figures 10, 11a and 11b). It should be borne in mind, however, that, as normalization is carried out for a particle in the forward direction, the proportion of particles traveling backward must be greater at high incident energies than at low ones.

Figures 12a, b and 13a and b show the angular distributions corresponding to $\pi(E_0, t, \Theta)$ and $\gamma(E_0, t, \Theta)$ at E_0 = 6 Gev and for several depths t.

V. Calculation of the primary energy from the path length of the electrons

Nagel has obtained the following expression for the mean overall

path length $\overline{S(E_0, 1.5)}$ of all the electrons in the cascade:

$$\overline{S(E_0, 1{,}5)} = 0{,}0905\ E_0 \pm 0{,}3\ \%\ [X_0]$$

having the half-width

$$\Delta S(E_0, 1{,}5) = 0{,}125 \sqrt{E_0}\ [X_0] .$$

We therefore obtain for $E_0 = 6$ Gev that

$$\overline{S(6\ \text{GeV}, 1{,}5)} = (543 \pm 1{,}5)\ X_0$$

$$\Delta S(6\ \text{GeV}, 1{,}5) = 9{,}7\ X_0$$

whilst the Monte Carlo method leads to

$$\overline{S(6\ \text{GeV}, 1{,}5\ )} = 545\ X_0$$
$$\Delta S(6\text{GeV}, 1{,}5) = 9\ X_0$$

VI. Spatial distribution of energy in the lead cylinder

In Nagel's system, the energy losses incurred during the cascade formation (the ionization losses of the electrons and the separation of particles below the cut-off energies) are represented in a spatial 'block diagram'. The expression $E(r,t)/E_0$ gives the percentage of the incident energy that is accumulated at a distance r from the cascade axis at a depth t in a cylindrical tube of height and thickness X_0 (i.e. in a volume of $2\pi r X_0^2$). Figure 14 shows the curves for

$$\left(\frac{E(r)}{E_0}\right)_{t=\infty} = \frac{1}{E_0}\int_0^\infty E(r,t')\,dt' \,, \quad \left(\frac{E(t)}{E_0}\right)_{r=\infty} = \frac{1}{E_0}\int_0^\infty E(r',t)\,dr'$$

and $$\left(\frac{1}{E_0}\int_t^\infty E(t')\,dt'\right)_{r=\infty} = \frac{1}{E_0}\int_t^\infty dt' \int_0^\infty dr'\; E(r',t')$$

The decrease for large t strictly obeys the $e^{-\lambda_{min} t}$ law.

We can calculate from the 'block diagram' the percentage of primary energy that leaves a lead cylinder with a given radius r and length t (in X_0) (see Figure 15). We must further add to the values shown in Figure 15 the energy that has been back-scattered to the plane of incidence, this energy amounting on average to 0.175%. It appears that no further gain occurs at a given length t, if r exceeds a maximum r(t).

Further, we can read off from the isoenergetic curves obtained the possible values of r and t necessary for the accumulation of a given percentage of energy in the lead cylinder. Nagel has found that these isoenergetic curves become, in a first approximation, independent of the primary energy E_0 when r is plotted against $t/\ln E_0$. Figure 16 shows Nagel's interpolated curves for 80, 90, and 93% of the incident

energy Nagel's points for 1000 Mev and our values for 6 Gev. It can be seen that the minimum length of t increases more slowly than ln E_0, and that the minimum radius decreases at higher energies. The cascade becomes, therefore, relatively narrow. Figure 16 also shows the curves for 98, 99, and 99.5% of incident energy (for E_0 = 6 Gev).

VI. Cascade produced by 6 Gev incident photons

The evaluation of 100 cascades produced by 6 Gev photons basically confirms the qualitative considerations as expressed e.g. by Heitler[4] (p. 393): A high energy photon leads to one pair formation after an average of 1.4 path lengths. After about 1 X_0, we have therefore the same initial conditions as in the case of an electron cascade in the plane of incidence. It follows therefore that a photon cascade is displaced in the direction of the cascade axis by about 1 X_0 with respect to the electron cascade. This is clearly shown by a comparison between Figures 1_γ, 2_γ and 14_γ on the one hand, and Figures 1, 2, and 14 on the other; the former set is generally similar to the latter.

Comparison of the radial distributions, the spectra, and the angular distributions shows that the distribution curve for $z = t.X_0$ in

the electron cascade approximately coincides with the distribution curve for $z = (t + 1)X_0$ in the photon cascade, particularly when t is large. However, differences arise for the first three or four path lengths. Furthermore, the energy back-scattered to the plane of incidence is 0.12% in the photon cascade, that is, less than in the electron cascade (0.175%).

The statistics are generally worse in the case of photon cascades (for the same number of cascades), since the 'fate' of the incident particles differs more here. A high-energy electron traversing a distance of $1\ X_0$ undergoes about 12 bremsstrahlung processes (distributed over the whole path) and loses on average two-thirds of its energy. On the other hand, a high-energy photon traverses a distance of $1\ X_0$ without incurring any energy loss, after which its energy is divided by pair formation (e^+-e^- pair).

R e f e r e n c e s

1. H.-H. Nagel and Ch. Schlier, Z.f. Phys. 174 (1963) 464.
2. H.-H. Nagel, Dissertation, Bonn 1964, Z.f. Phys. 186 (1965) 319.
3. H.-H. Nagel, Z.f. Phys. 186 (1965) 319 and private communication.
4. W. Heitler, Quantum Theory of Radiation, Oxford, 3rd Ed., p.392.
5. K. Ott, Z. Naturf. 9a (1954) 488.

E (MeV)	Π_{max} Monte Carlo	Π_{max} from (1a)	Π_{max} from (1')	$t_{max}(\pi)[X_o]$ Monte Carlo	$t_{max}(\pi)$ from (2)	$t_{max}(\pi)$ from (2')
1,5	34	38,85	34,2	5,5	5,65	(7,2)
3,0	30	35,2	31	5,5	5,48	(6,5)
6,0	25,5	29,65	26,1	5,0	5,27	(5,8)
10,0	21,3	24,55	21,6	4,8	5,18	(5,3)
20,0	15	17,2	15,2	4,5	4,9	4,6
30,0	11,6	13,25	11,7	4,2	4,6	4,2
40,0	9,5	10,85	9,58	4,0	4,3	3,9
50,0	8,0	9,2	8,13	3,8	3,9	3,68
80,0	5,5	6,37	5,65	3,3	--	3,2
100,0	4,6	5,31	4,72	3,0	--	3,0
200,0	2,7	2,93	2,71	2,4	--	2,3
400,0	1,6	1,78	1,72	1,4	--	1,6
1000,0	1,05	0,99	0,93	0,8	--	0,7

TABELLE I : $\Pi_{max}(E_o, E)$, $t_{max}(\pi)(E_o, E)$ for E_o = 6 GeV

E (MeV)	T_{max} Monte Carlo	T_{max} from (3)	T_{max} from (3')	t_{max} (γ) Monte Carlo	t_{max} (γ) from (4)	t_{max} (γ) from (4')
0,25	332	370	333	7,8		
1,0	245	260	234	7,8		
1,5	200	224	201	7,7		7,9
2,0	168	181	163	7,5		7,6
3,0	129	140	126	7,3		7,2
5,0	89,1	113	102	7,0		6,7
10	49,3	53,8	48,5	6,0	(8,3)	6,0
20	26,4	28,9	26,1	5,5	6,4	5,3
30	17,8	19,8	17,9	4,8	5,5	4,9
40	13,6	15,1	13,6	4,5	4,9	4,6
60	9,33	10,4	9,4	4,0	4,2	4,2
80	7,26	7,9	7,1	3,5	3,8	3,9
100	5,90	6,5	5,85	3,2	3,5	3,7
200	3,4	3,5	3,15	2,4	2,7	
300	2,4	2,45	2,25	2,1	2,3	
400	1,9	(1,95)	1,80	1,8	2,1	
600	1,27	(1,50)	1,40	1,6	1,8	
800	0,92	(1,20)	1,13	1,6	1,6	
1000	0,76	(1,05)	0,99	1,5	1,5	
2000	0,36		0,72	1,0	1,1	
3000	0,21		0,63	0,5	(0,94)	

TABELLE II: T_{max} (E_o, E), $t_{max(\gamma)}$ (E_o, E) for E_o = 6 GeV

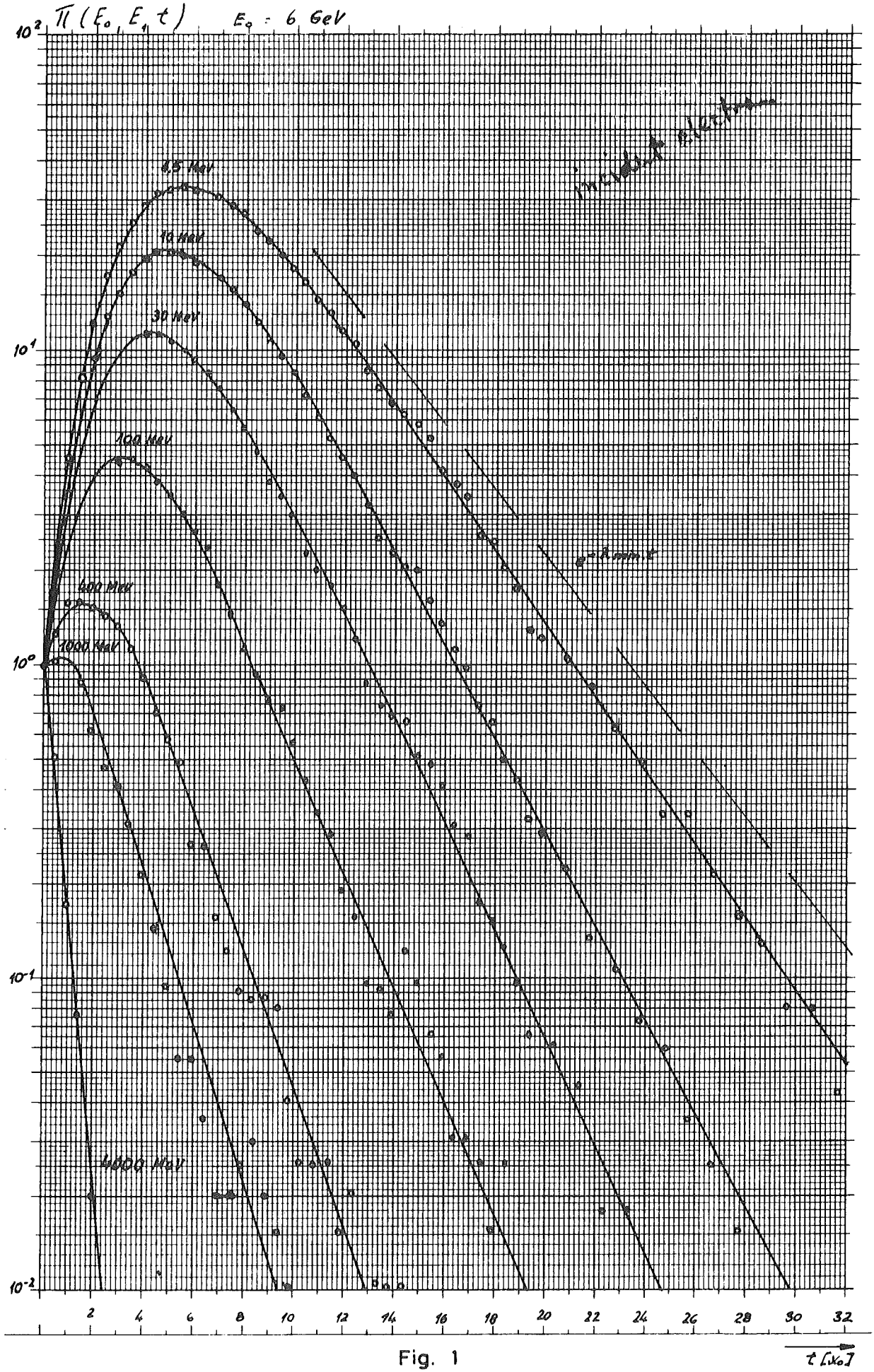
$\Pi(E_0, E, t)$
$E_0 = 6$ GeV
4,5 MeV
10 MeV
30 MeV
100 MeV
400 MeV
1000 MeV
4800 MeV
$e^{-\lambda_{min} t}$
10^2
10^1
10^0
10^{-1}
10^{-2}
2
4
6
8
10
12
14
16
18
20
22
24
26
28
30
32
t [x0]

Fig. 1

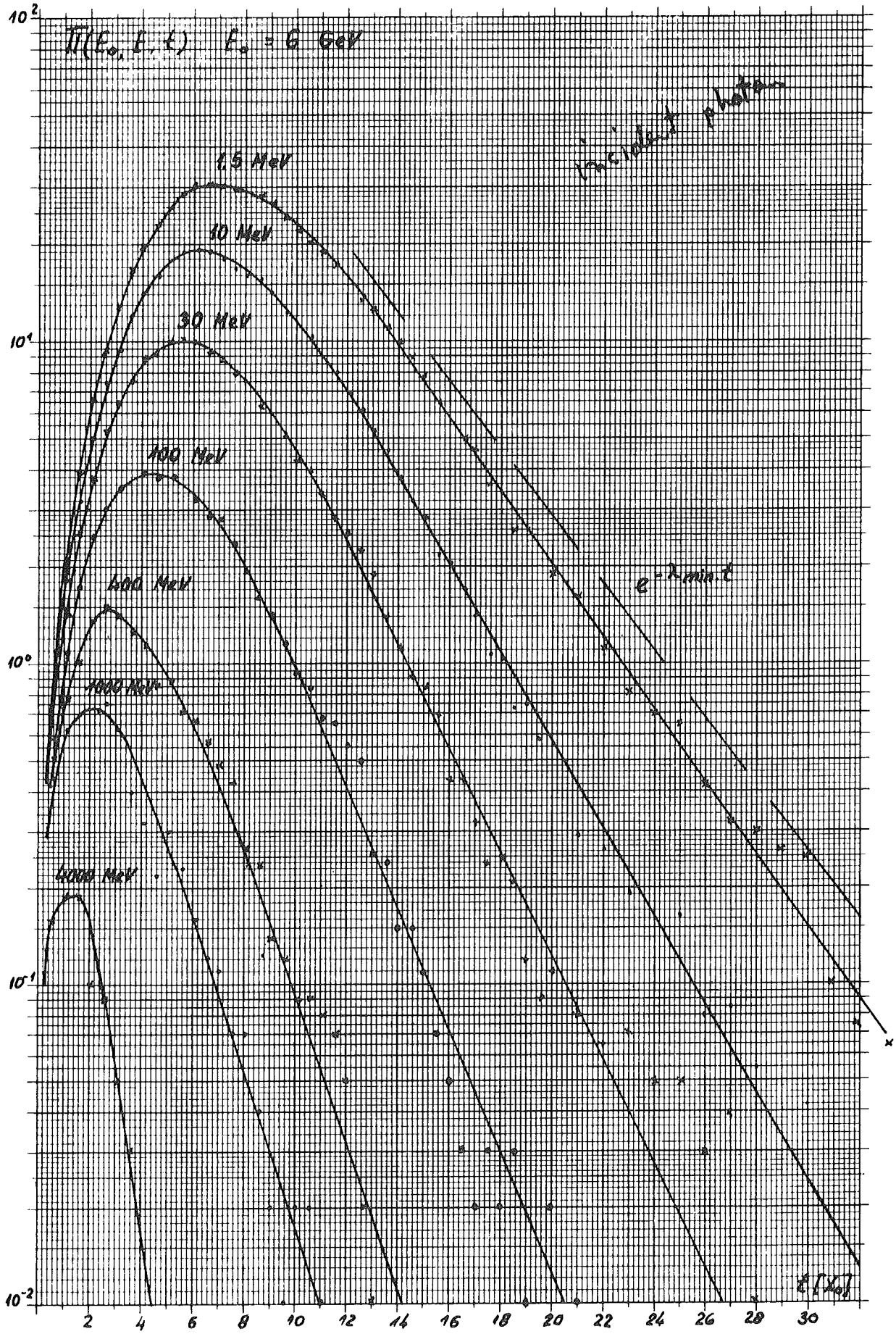
$\Pi(E_0, E, t)$ $E_0 = 6$ GeV
1.5 MeV
10 MeV
30 MeV
100 MeV
300 MeV
1000 MeV
3000 MeV
$e^{-\lambda_{min} t}$
10^2
10^1
10^0
10^{-1}
10^{-2}
2
4
6
8
10
12
14
16
18
20
22
24
26
28
30
x

Fig 1γ

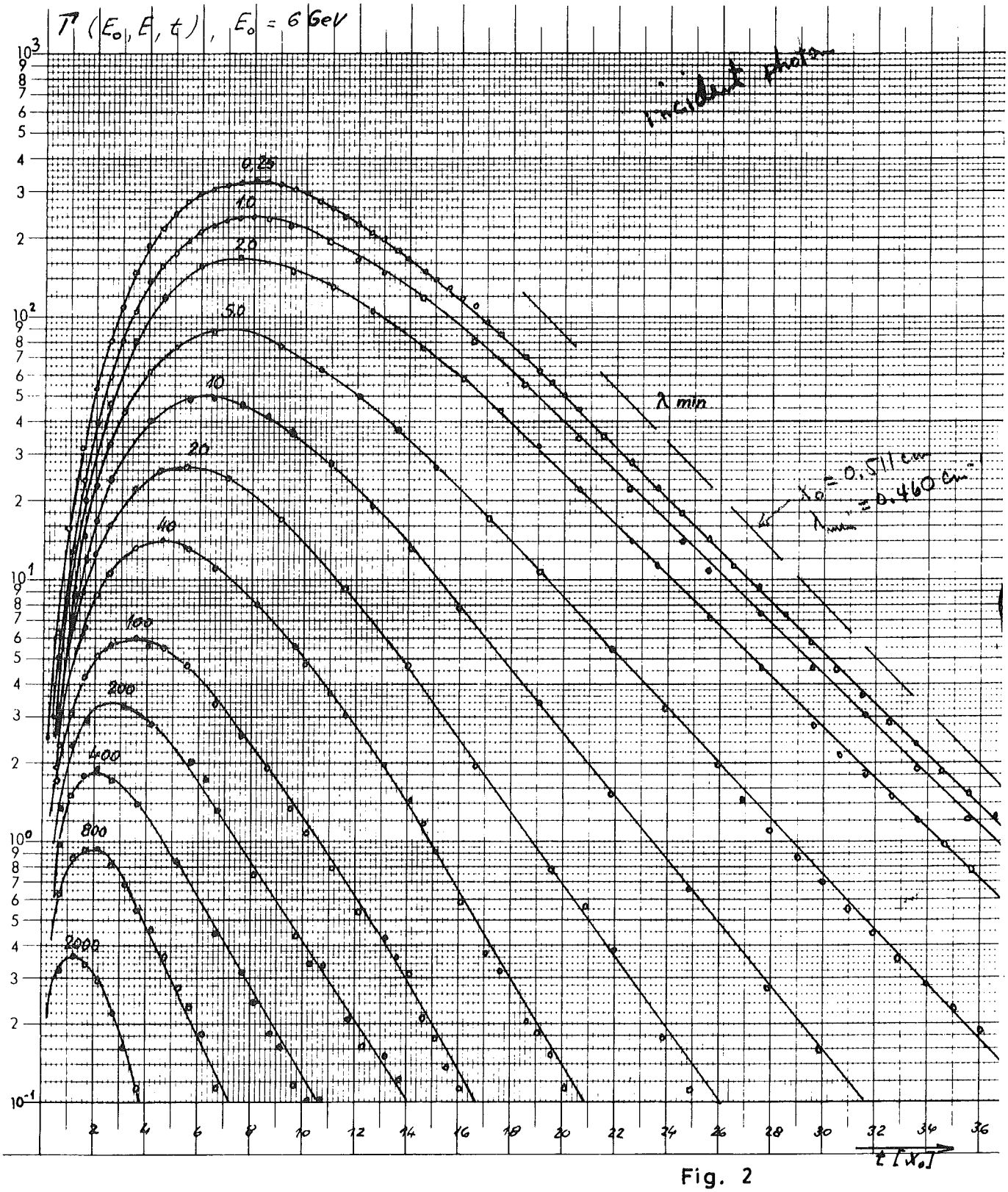
$T^{\gamma}(E_0, E, t)$, $E_0 = 6$ GeV
0.25
1.0
2.0
5.0
10
20
40
100
200
400
800
2000
λ min
$X_0 = 0.511$ cm
$\lambda_{min} = 0.460$ cm
$t\ [X_0]$

Fig. 2

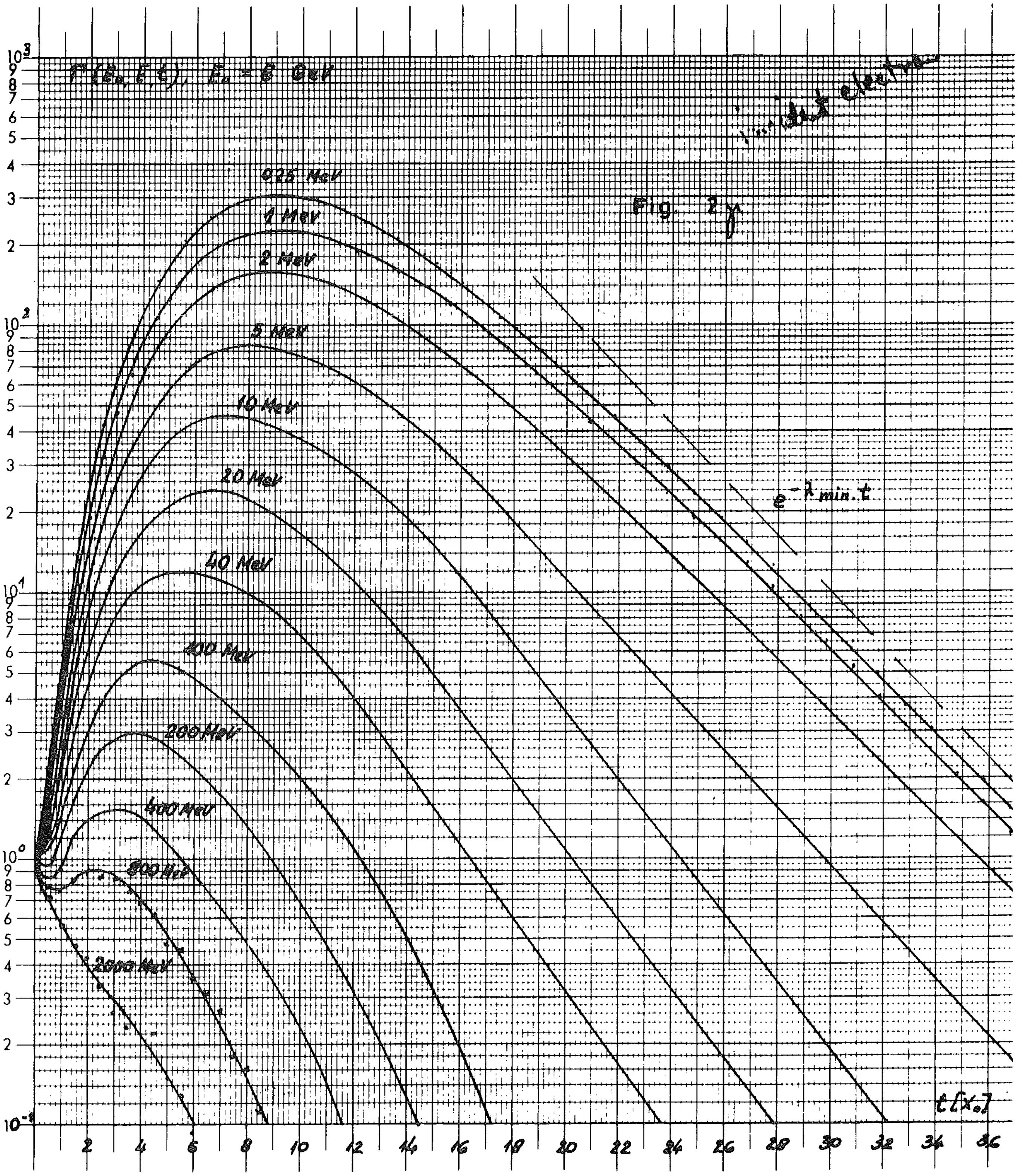
Γ(E₀, E, t), E₀ = 6 GeV
Fig. 2γ
0.25 MeV
1 MeV
2 MeV
5 MeV
10 MeV
20 MeV
40 MeV
100 MeV
200 MeV
400 MeV
800 MeV
2000 MeV
e^{-λ min. t}
t [X₀]
10³
10²
10¹
10⁰
10⁻¹
2
4
6
8
10
12
14
16
18
20
22
24
26
28
30
32
34
36

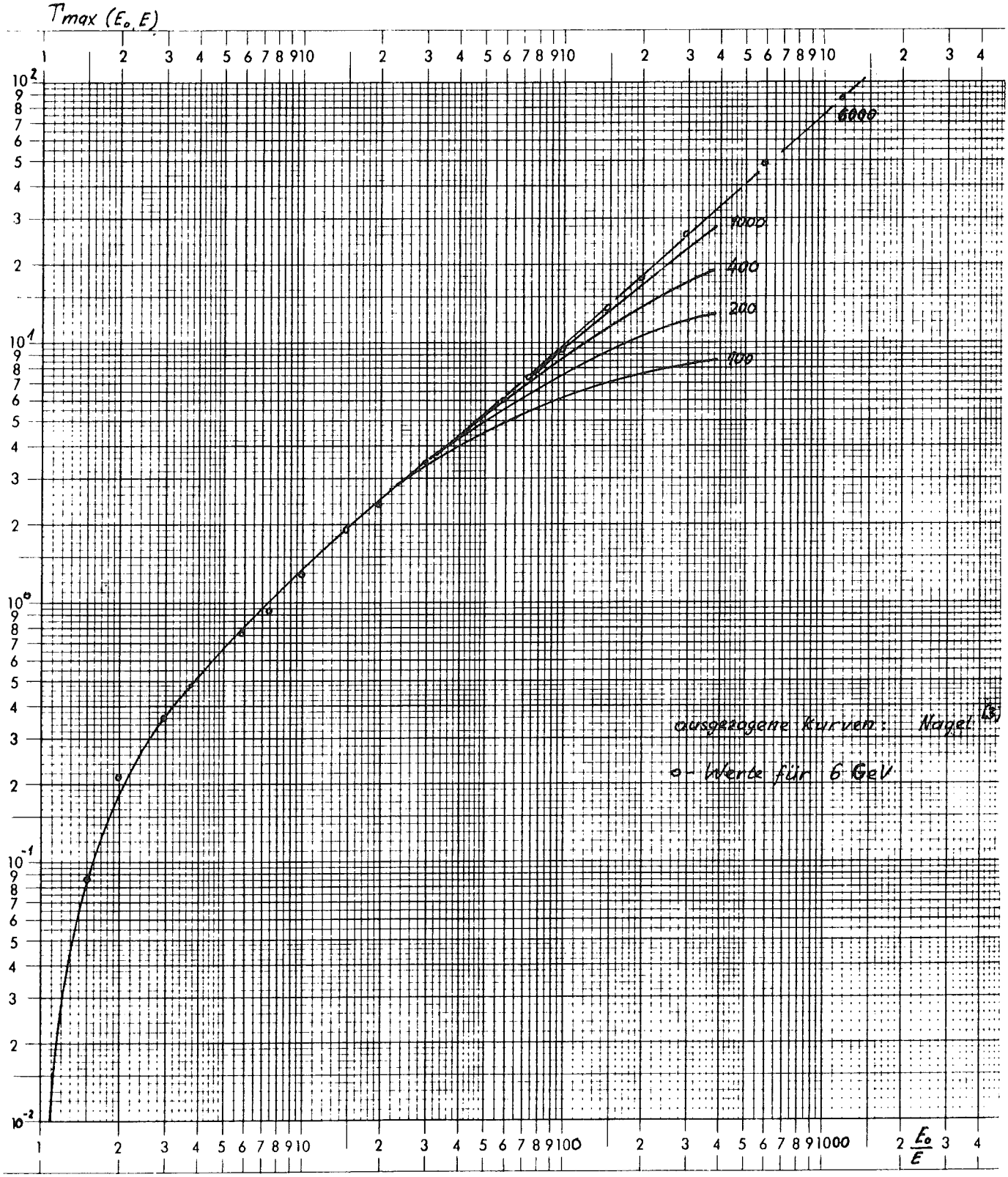
$T_{max}(E_0, E)$
6000
1000
400
200
100
ausgezogene Kurven: Nagel [45]
σ - Werte für 6 GeV
$\frac{E_0}{E}$

Fig. 3

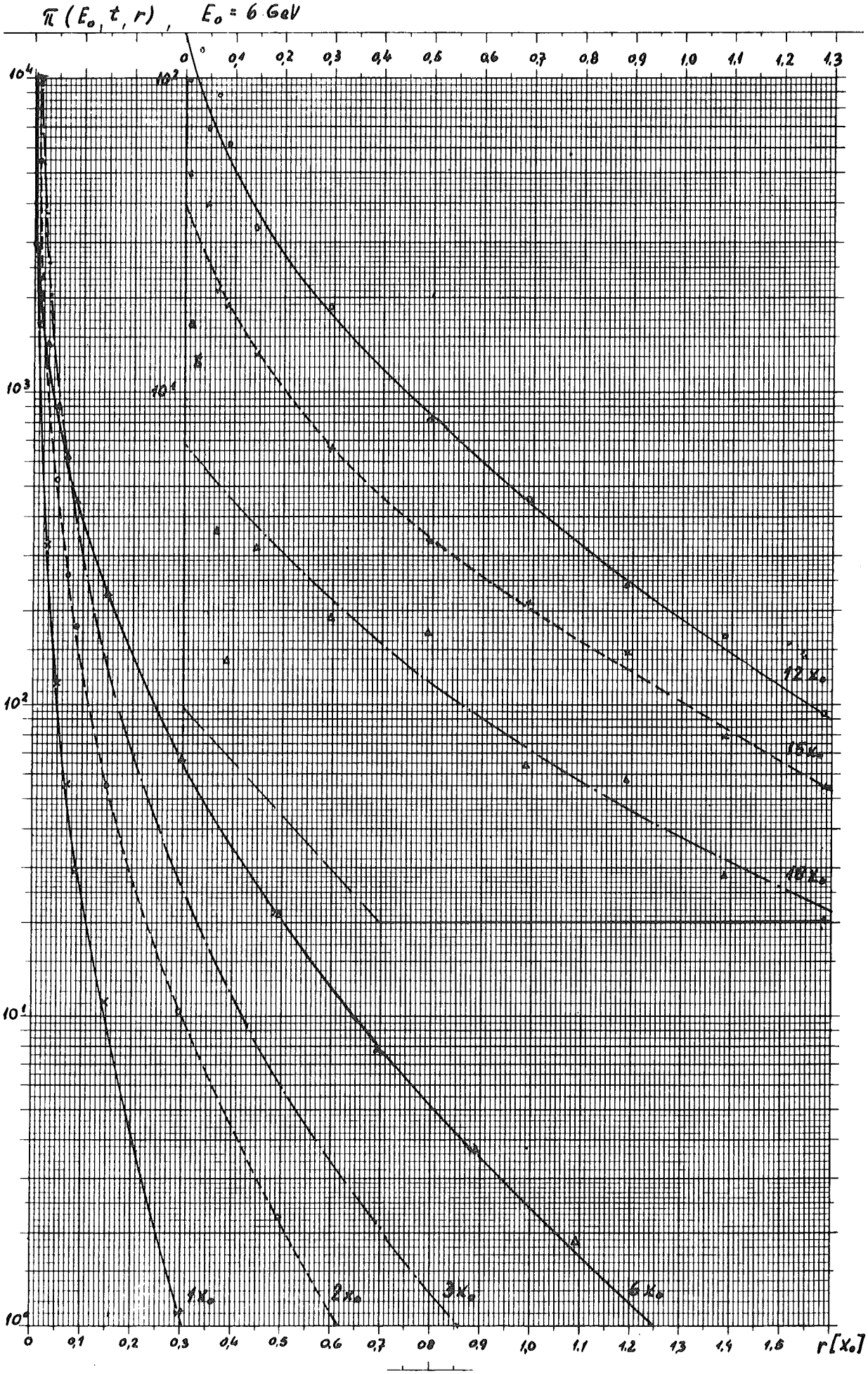
π (E₀, t, r), E₀ = 6 GeV
0 0,1 0,2 0,3 0,4 0,5 0,6 0,7 0,8 0,9 1,0 1,1 1,2 1,3
10⁴
10³
10²
10¹
10⁰
1 X₀
2 X₀
3 X₀
6 X₀
12 X₀
15 X₀
18 X₀
0 0,1 0,2 0,3 0,4 0,5 0,6 0,7 0,8 0,9 1,0 1,1 1,2 1,3 1,4 1,5 r [X₀]

Fig. 4

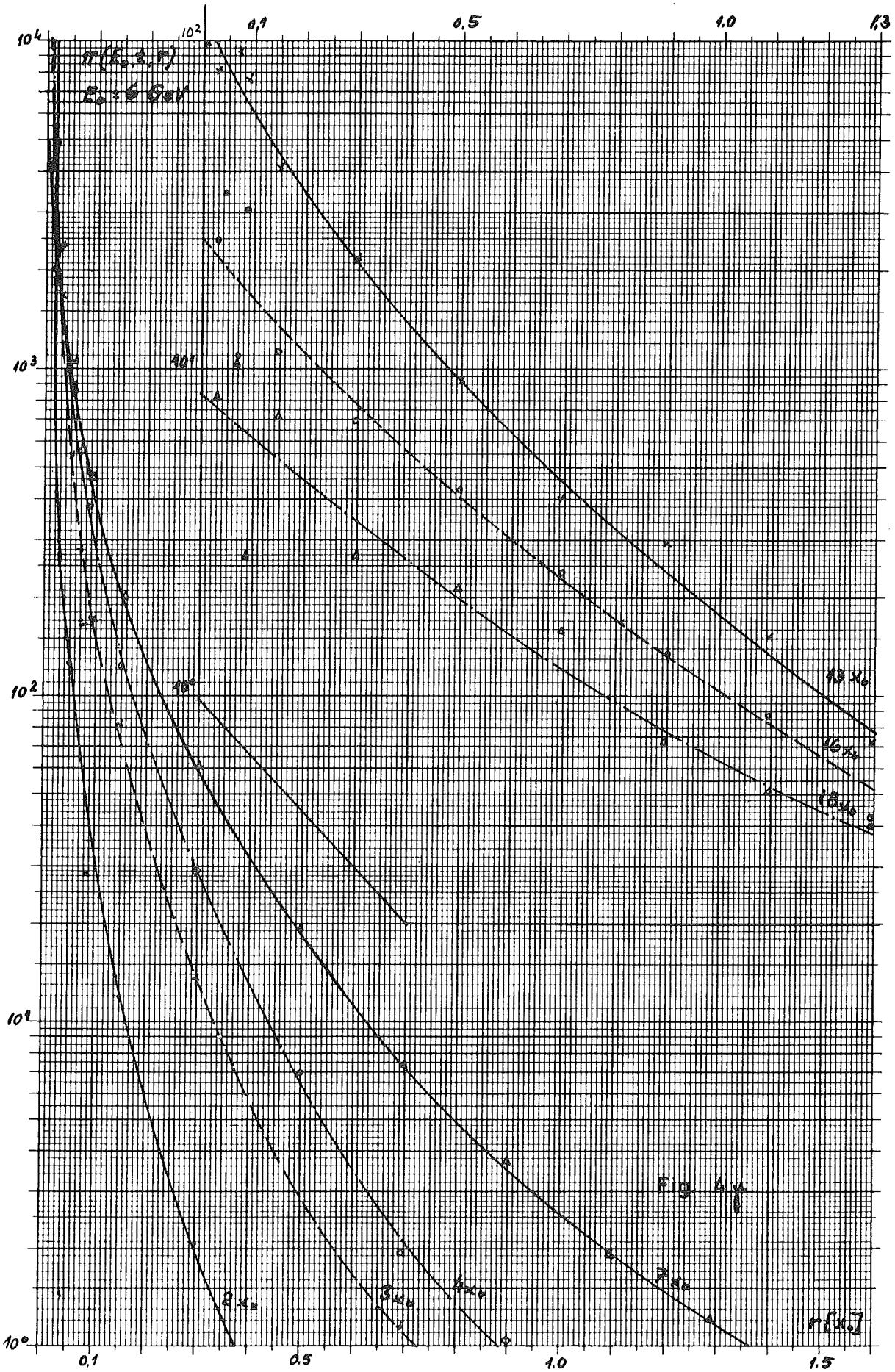
$\pi(E_0, t, r)$
$E_0 = 6$ GeV
10^4
10^3
10^2
10^1
10^0
0,1
0,5
1,0
1,3
1,5
2 X_0
3 X_0
6 X_0
9 X_0
13 X_0
16 X_0
18 X_0
$t[X_0]$

Fig. 4

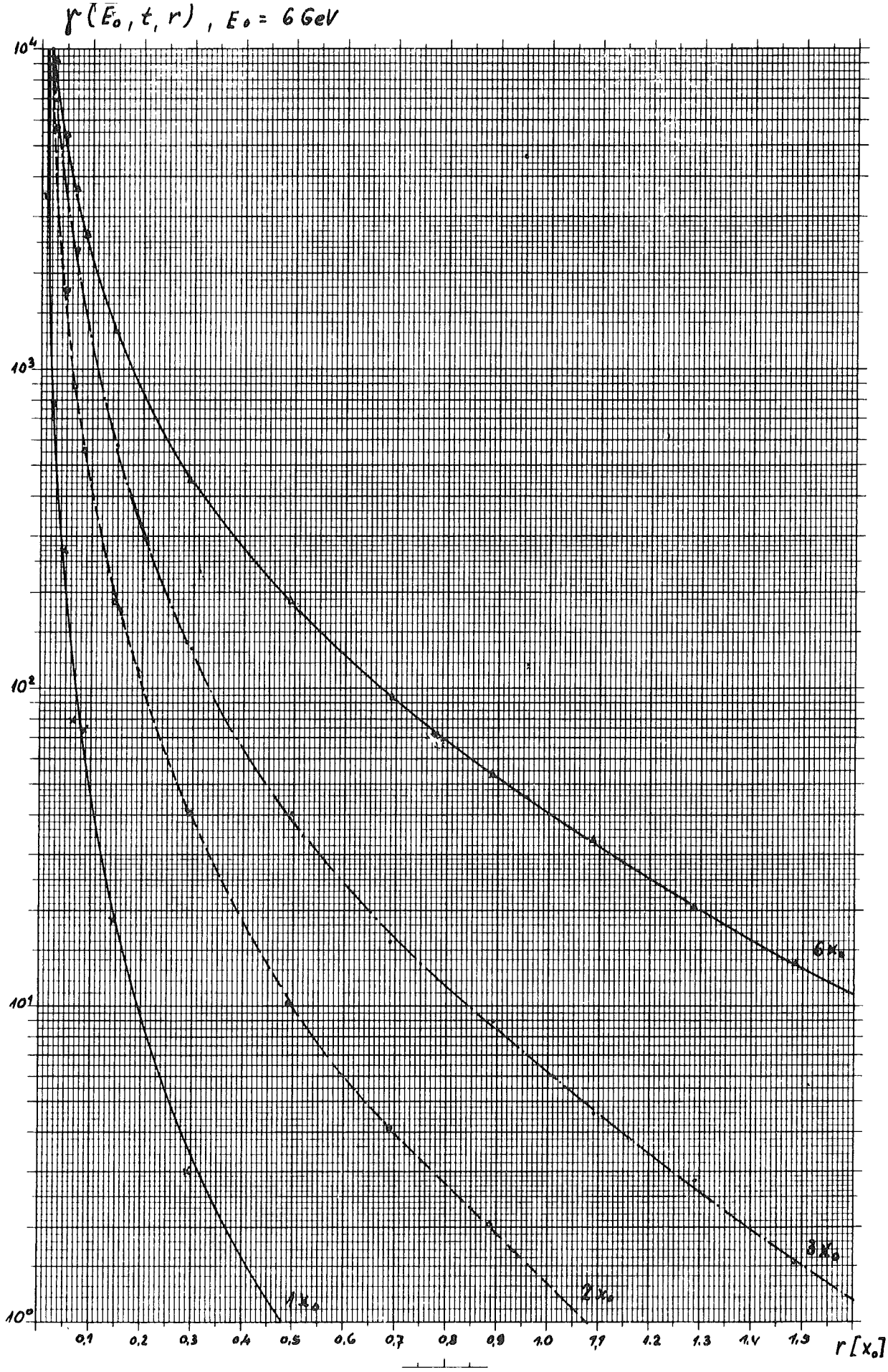
γ(E₀, t, r) , E₀ = 6 GeV
10⁴
10³
10²
10¹
10⁰
0,1
0,2
0,3
0,4
0,5
0,6
0,7
0,8
0,9
1,0
1,1
1,2
1,3
1,4
1,5
r [X₀]
6X₀
3X₀
2X₀
1X₀

Fig. 5a

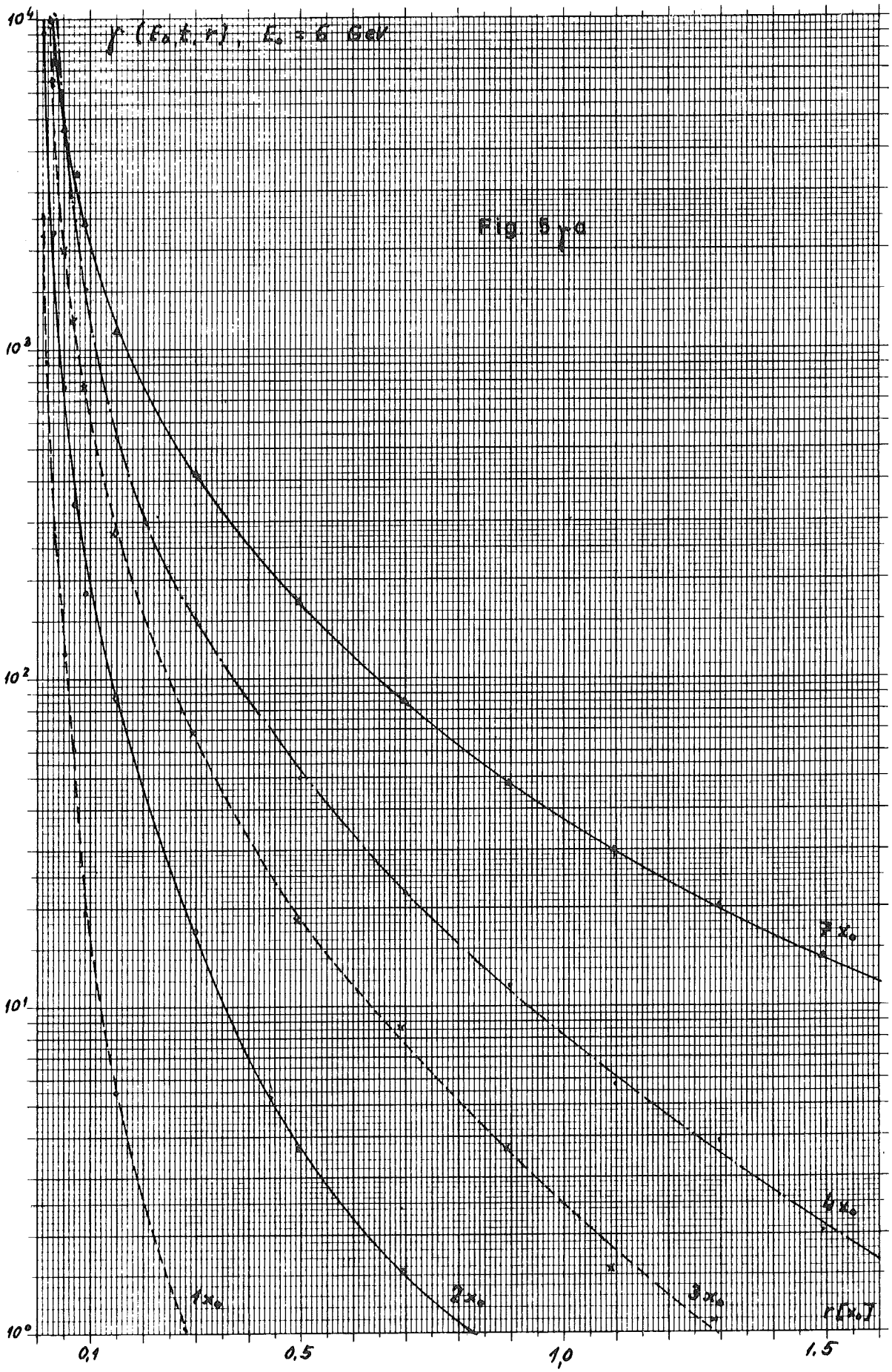
$f(t_0, t, r)$, $E_0 = 6$ GeV
10^4
10^3
10^2
10^1
10^0
0,1
0,5
1,0
1,5
$1 x_0$
$2 x_0$
$3 x_0$
$4 x_0$
$5 x_0$
r[x.]

Fig 6 γa

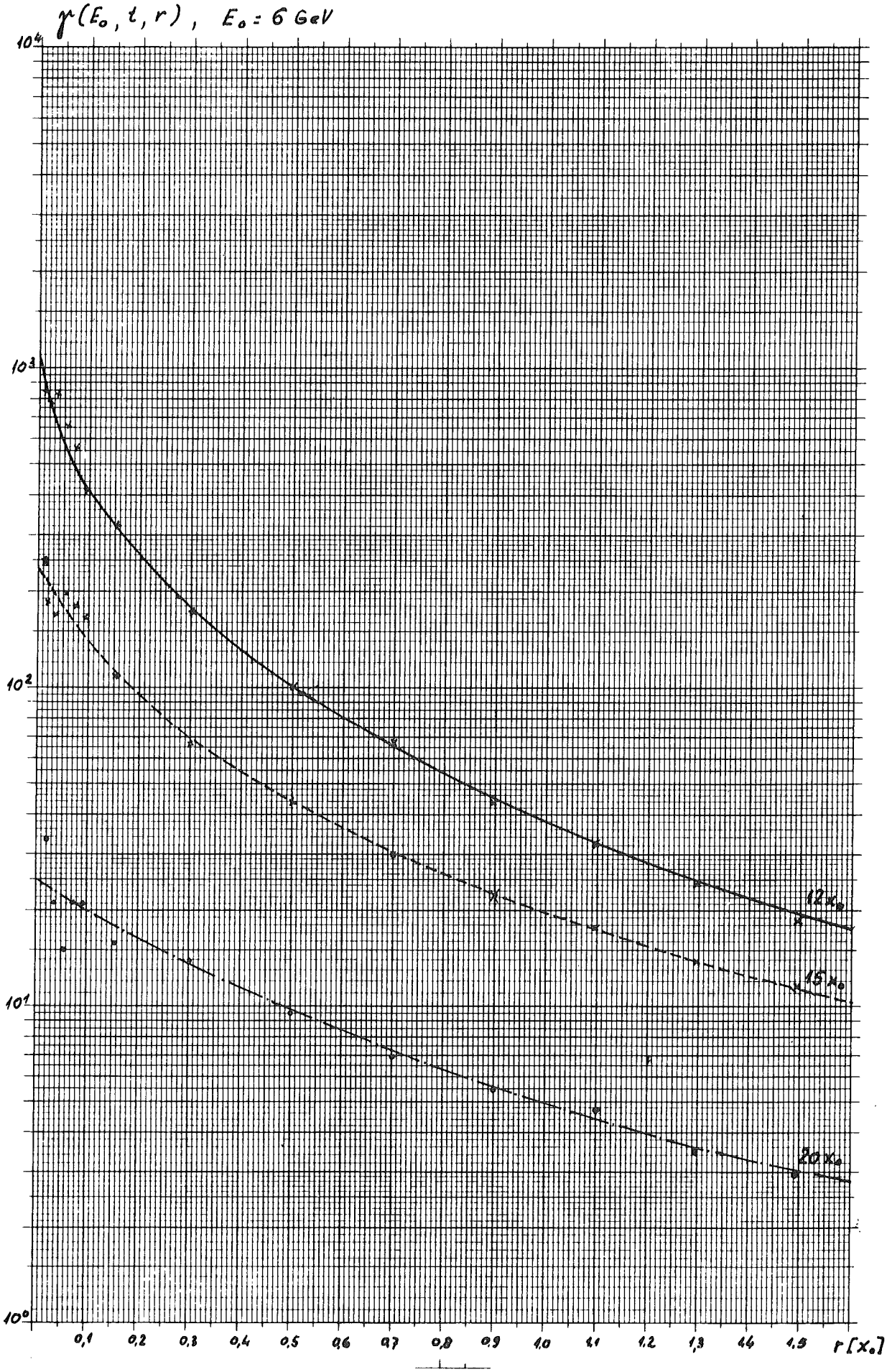
γ(E₀, t, r), E₀ = 6 GeV
10⁴
10³
10²
10¹
10⁰
12 X₀
15 X₀
20 X₀
0,1
0,2
0,3
0,4
0,5
0,6
0,7
0,8
0,9
1,0
1,1
1,2
1,3
1,4
1,5
r [X₀]

Fig. 5 b

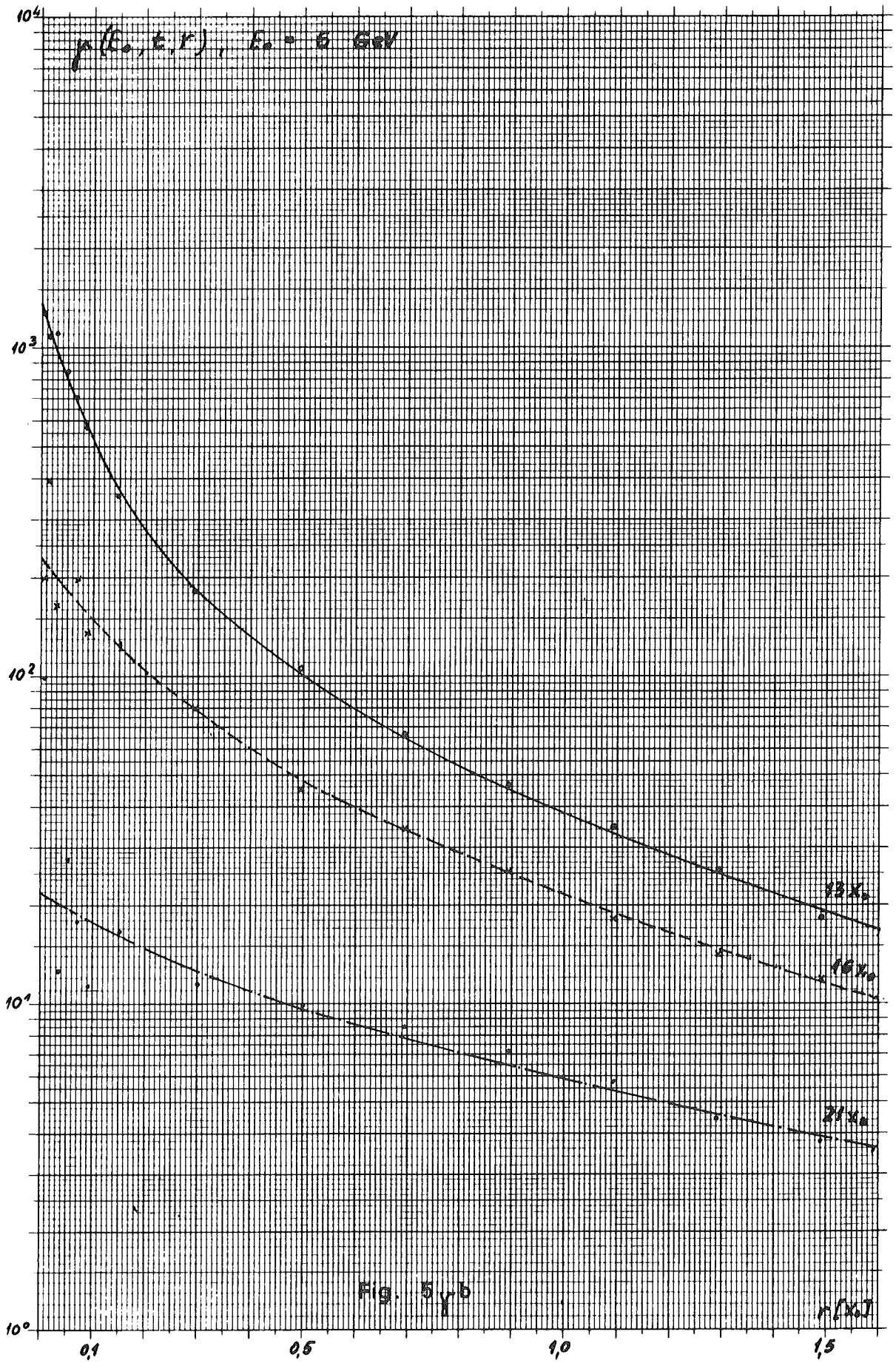

Fig. 5 γ b

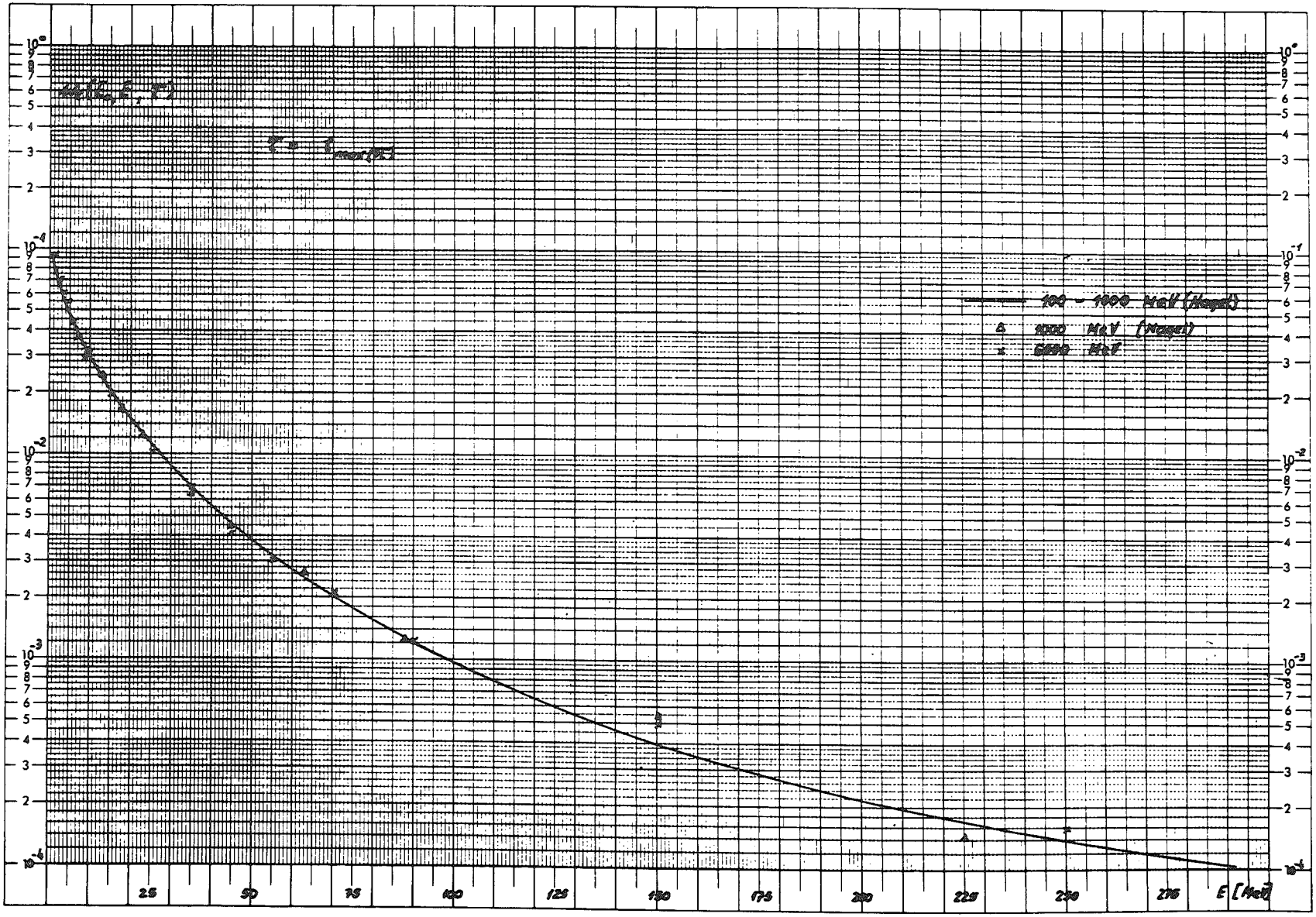

Fig. 6a

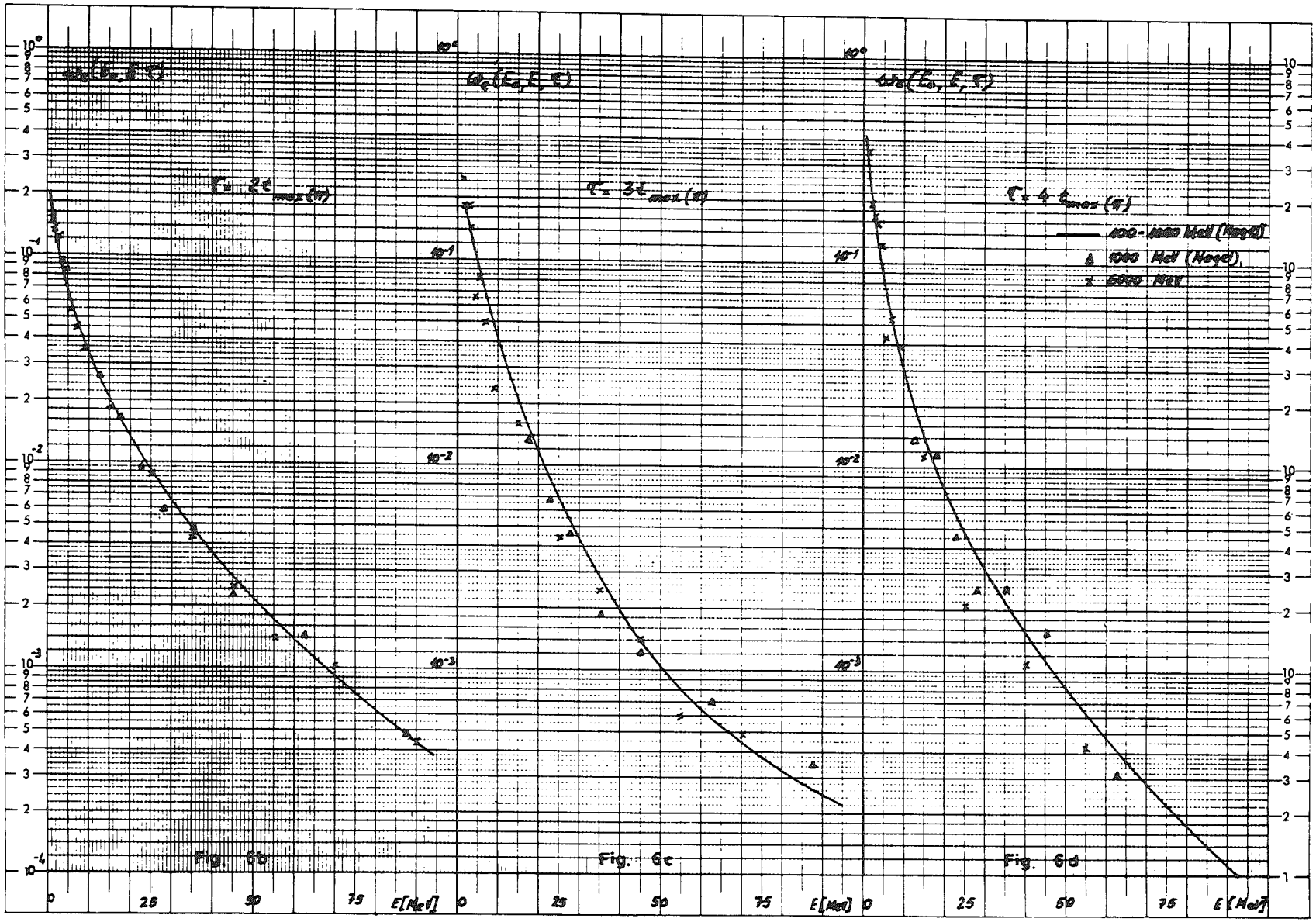

Fig. 6b Fig. 6c Fig. 6d

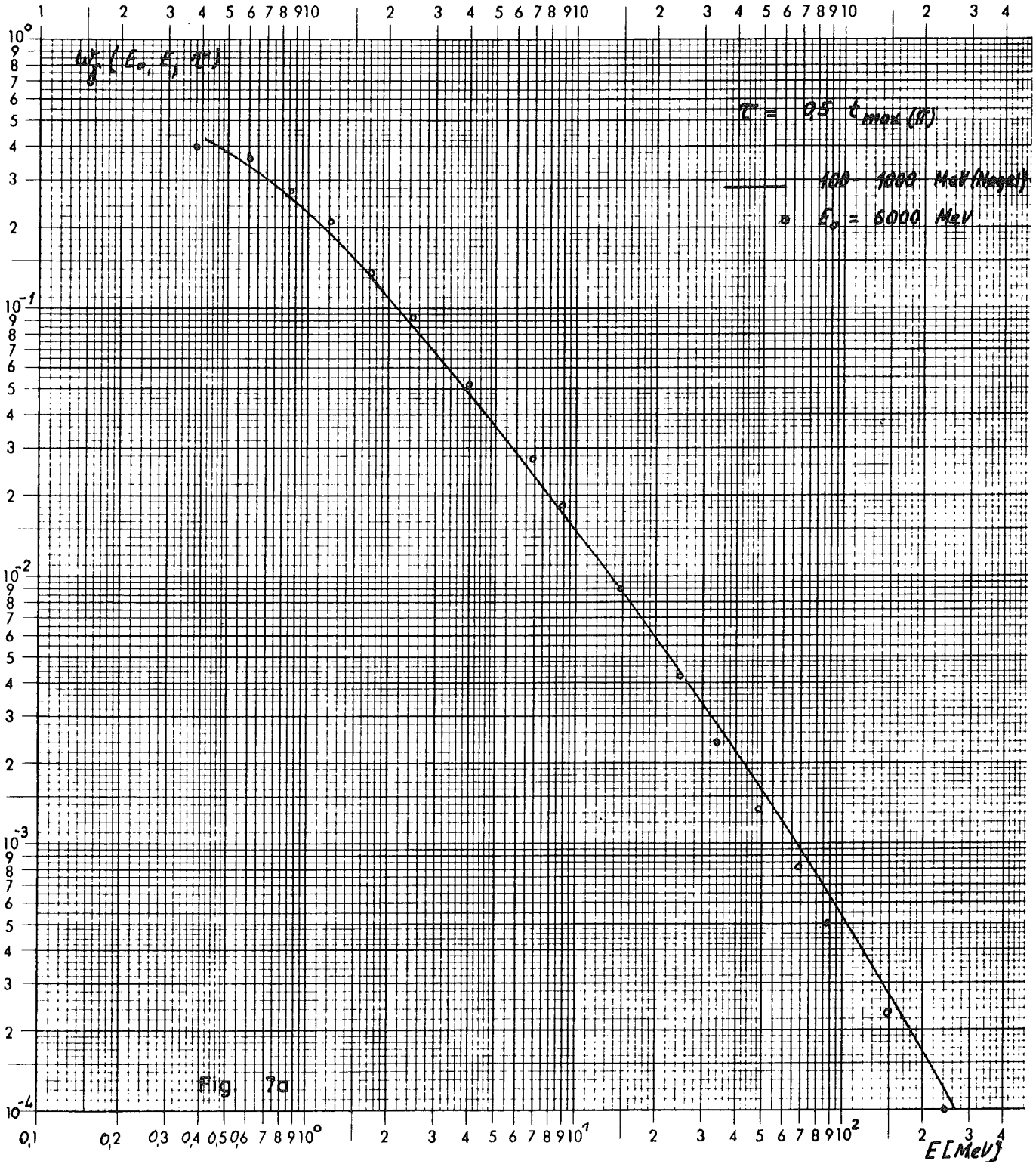
$w_\gamma(E_0, E, \tau)$
$\tau = 0.5\ t_{max}(E)$
100 - 1000 MeV (Nagel)
$E_0 = 6000$ MeV
E [MeV]

Fig. 7a

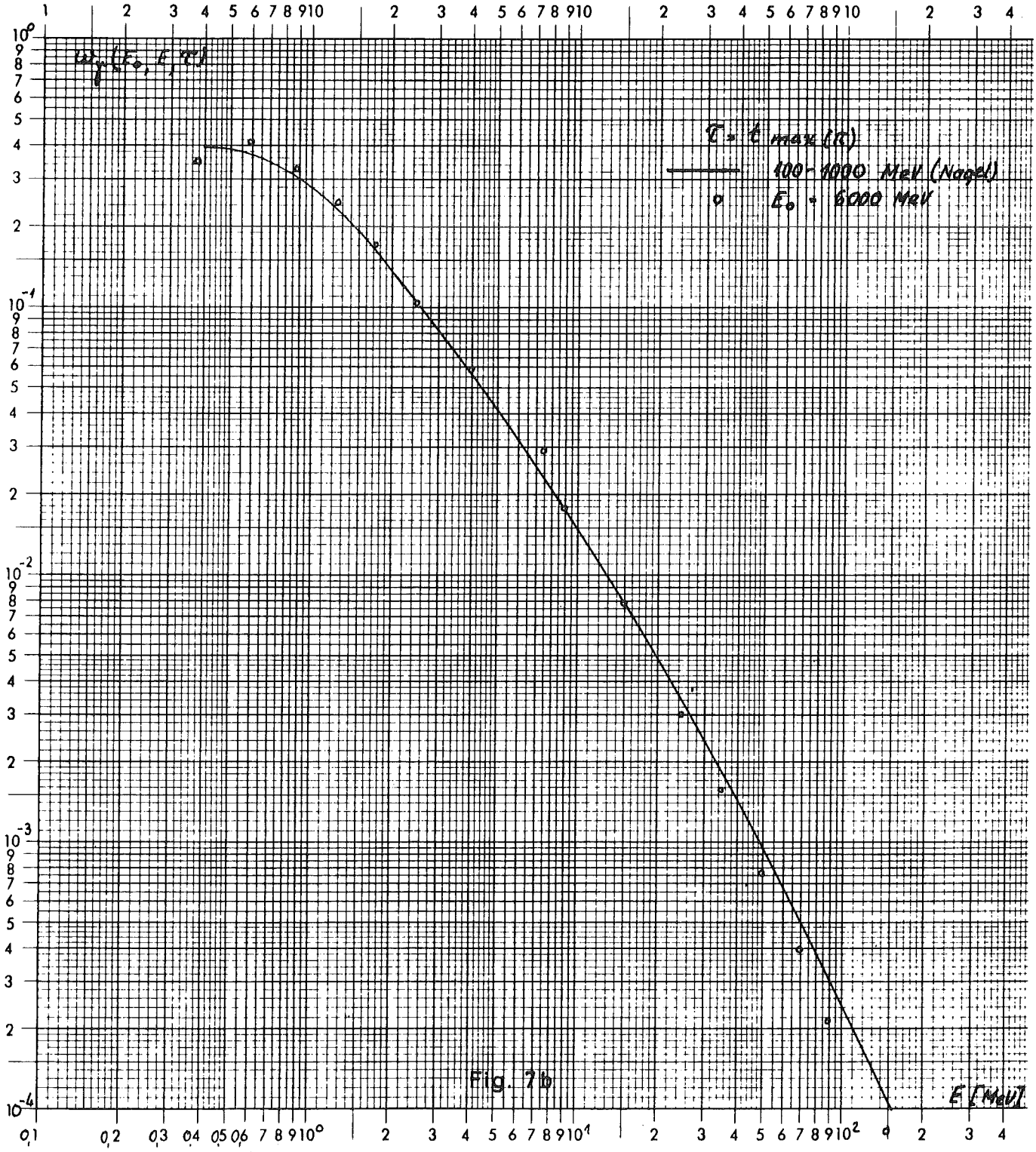
$W_\gamma(E_0, E, \alpha)$
$\alpha = \alpha_{max}(E)$
100 - 1000 MeV (Nagel)
E_0 = 6000 MeV
E [MeV]

Fig. 7b

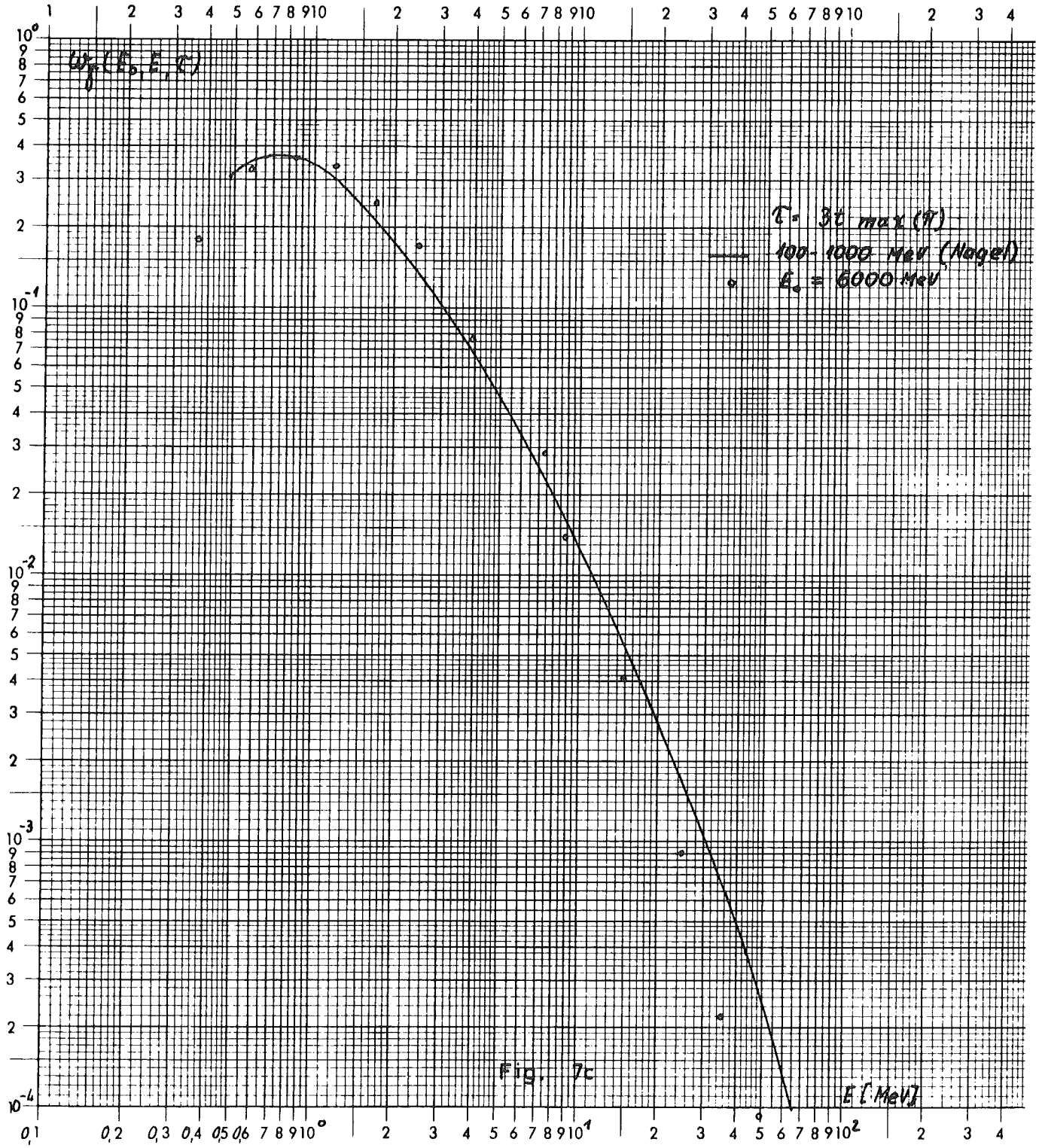

Fig. 7c

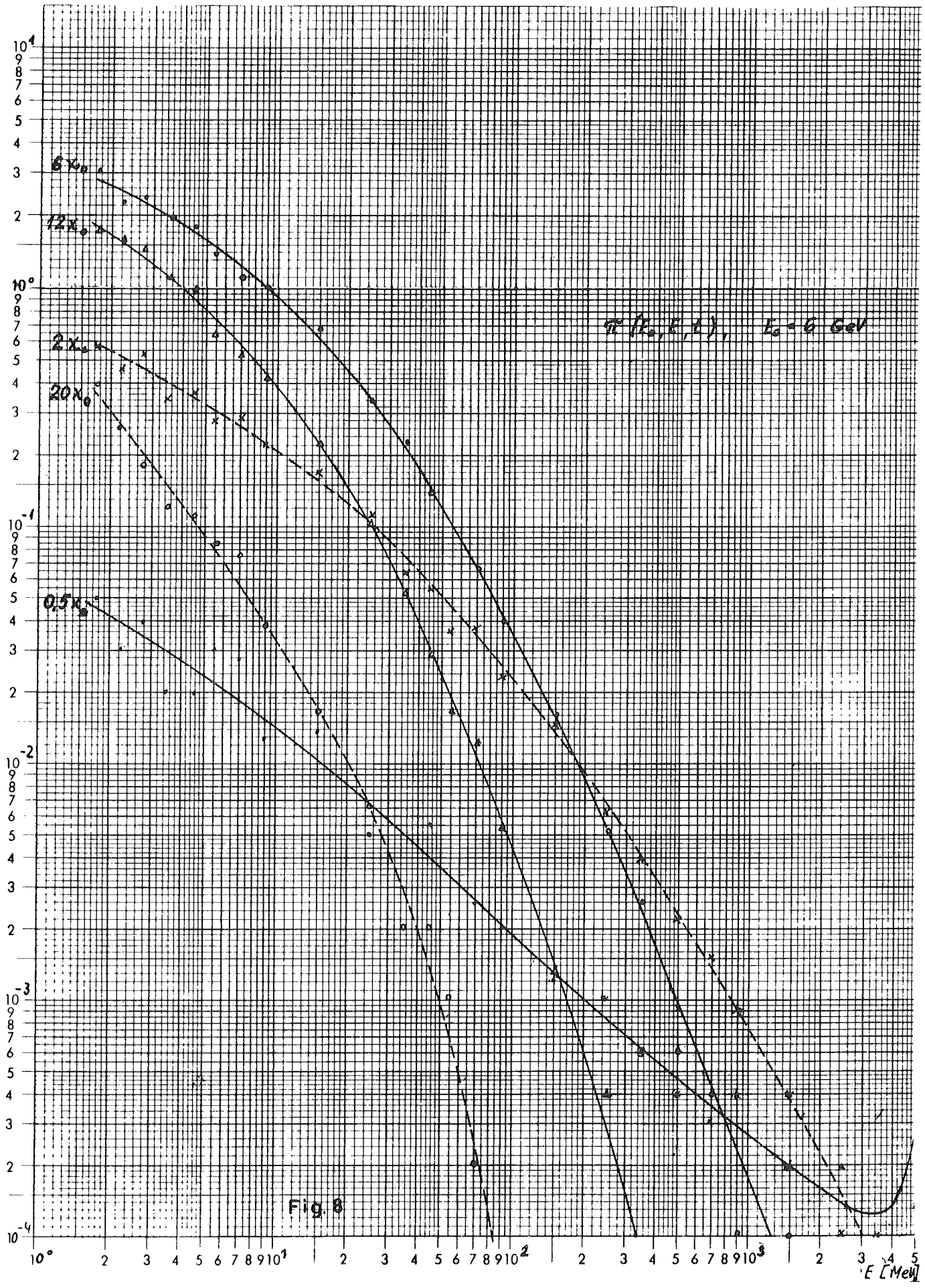

Fig. 8

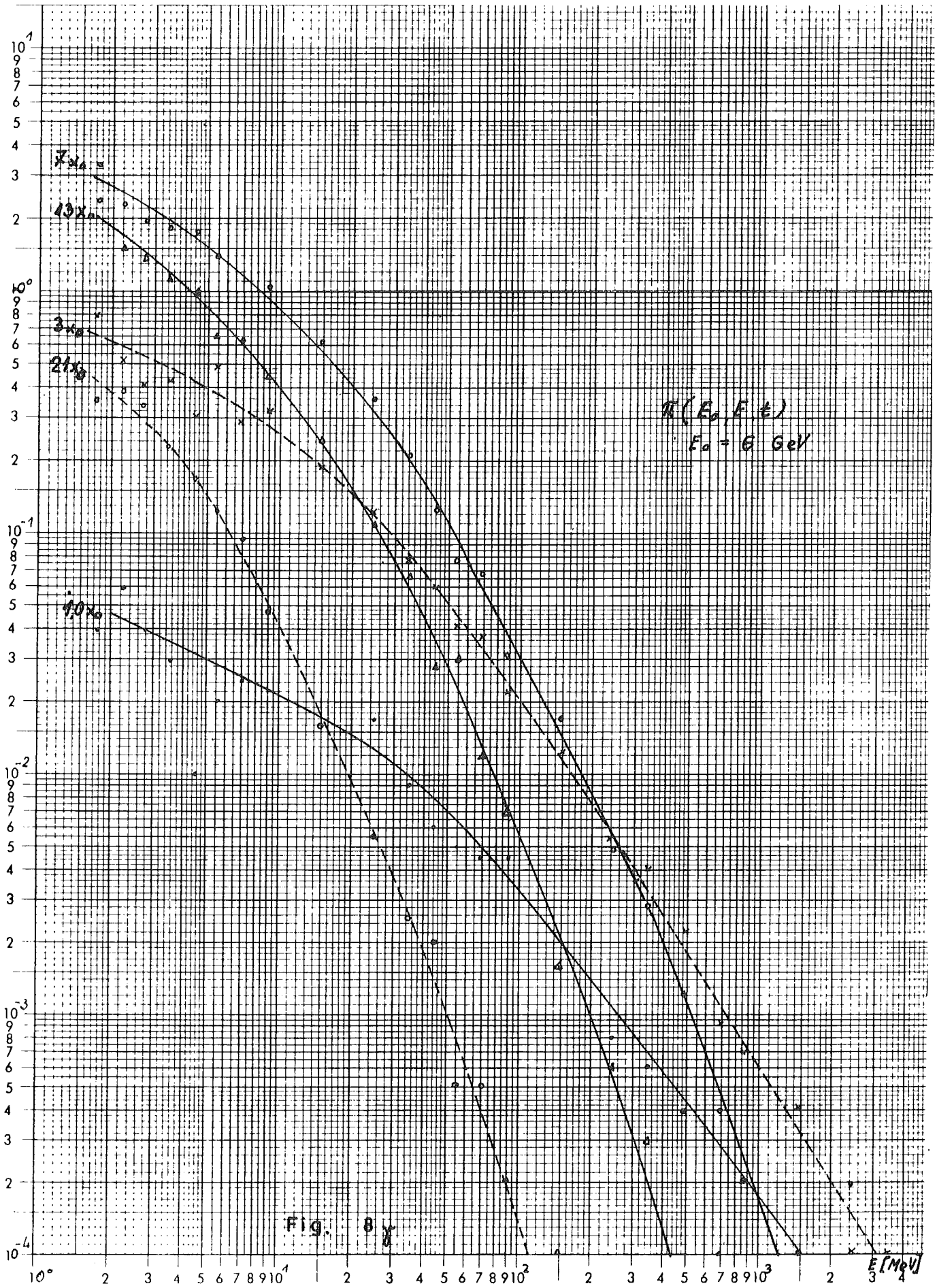

Fig. 8

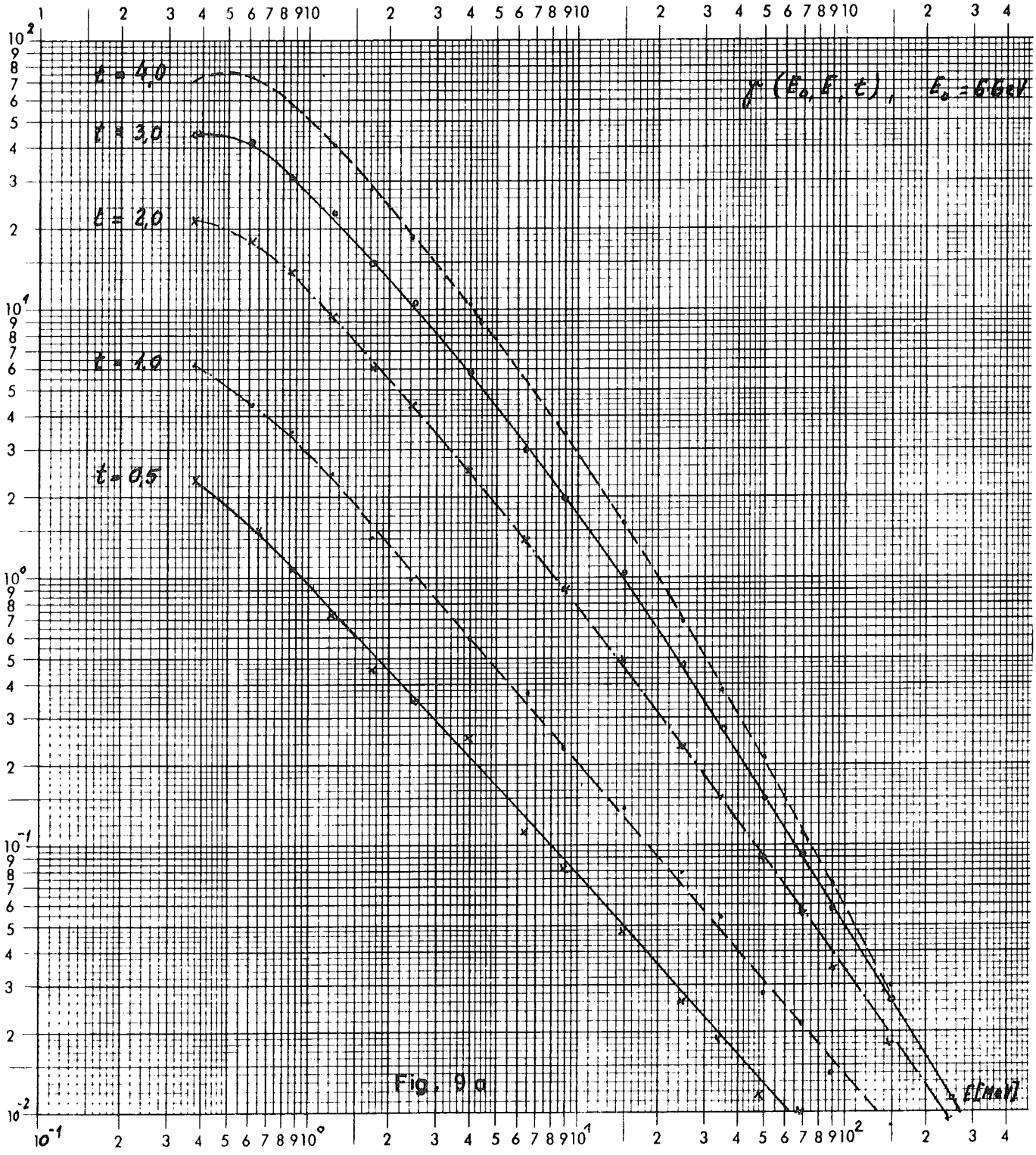

Fig. 9 a

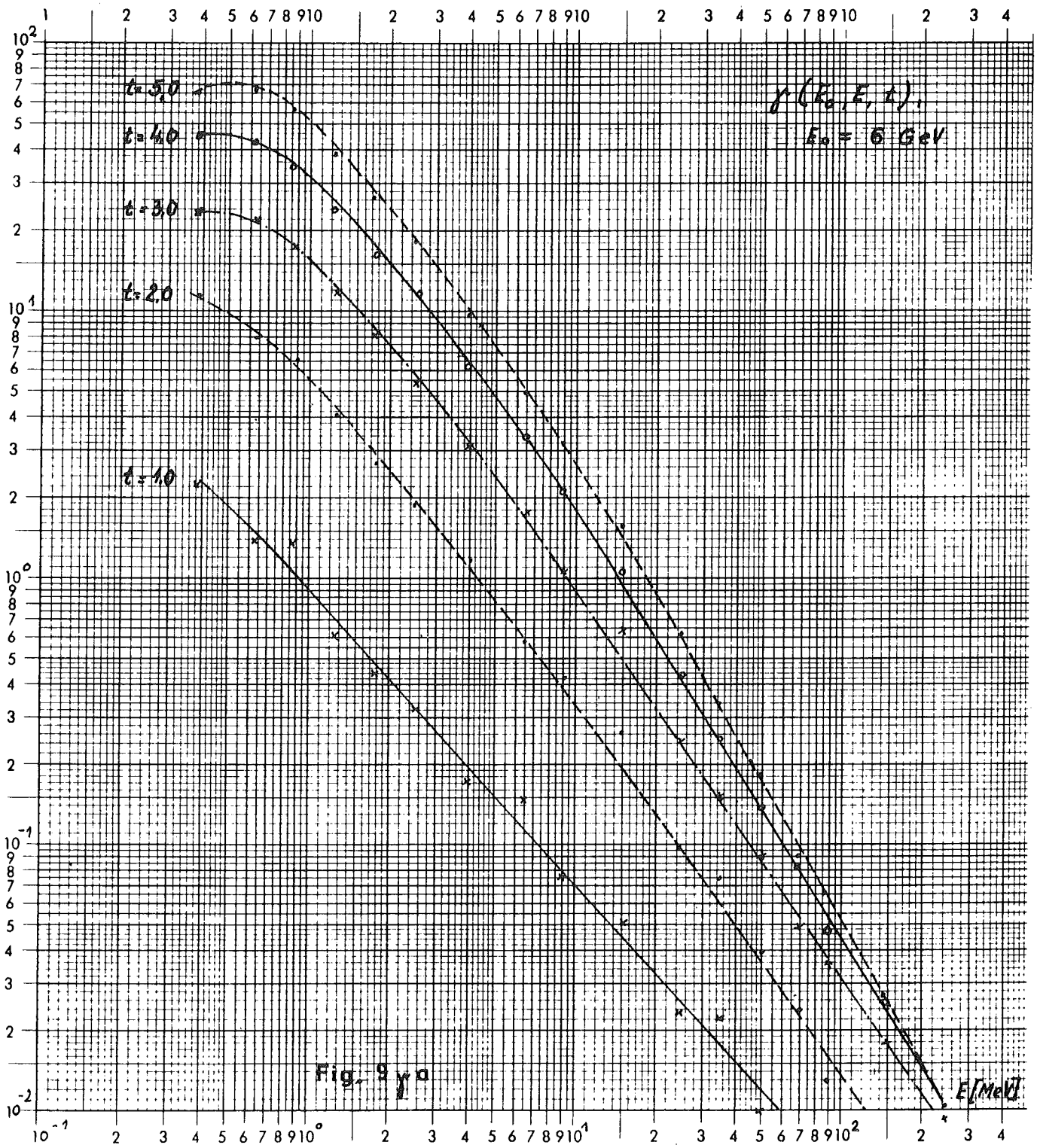

Fig. 9 γ a

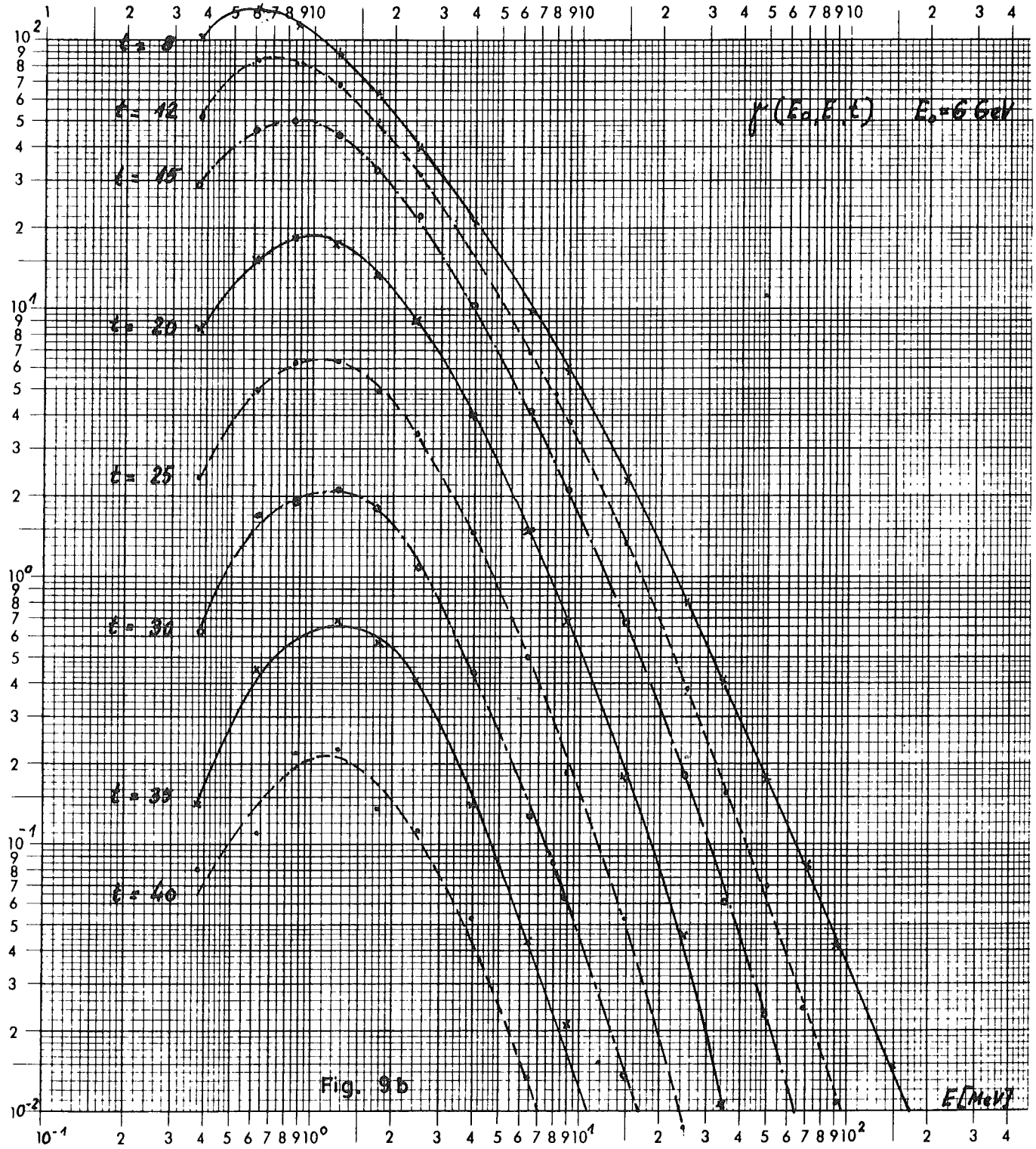

Fig. 9b

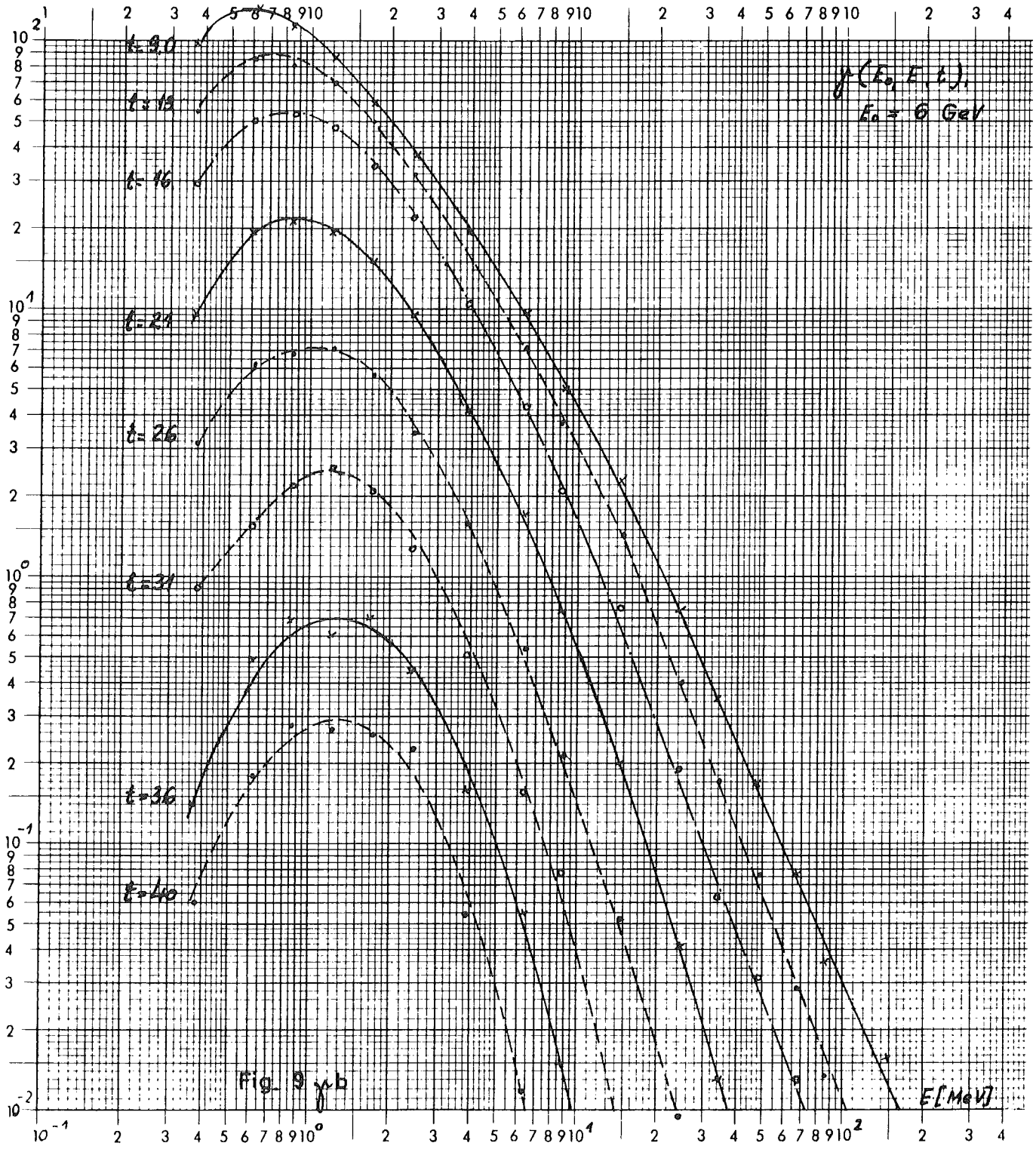

Fig. 9 γb

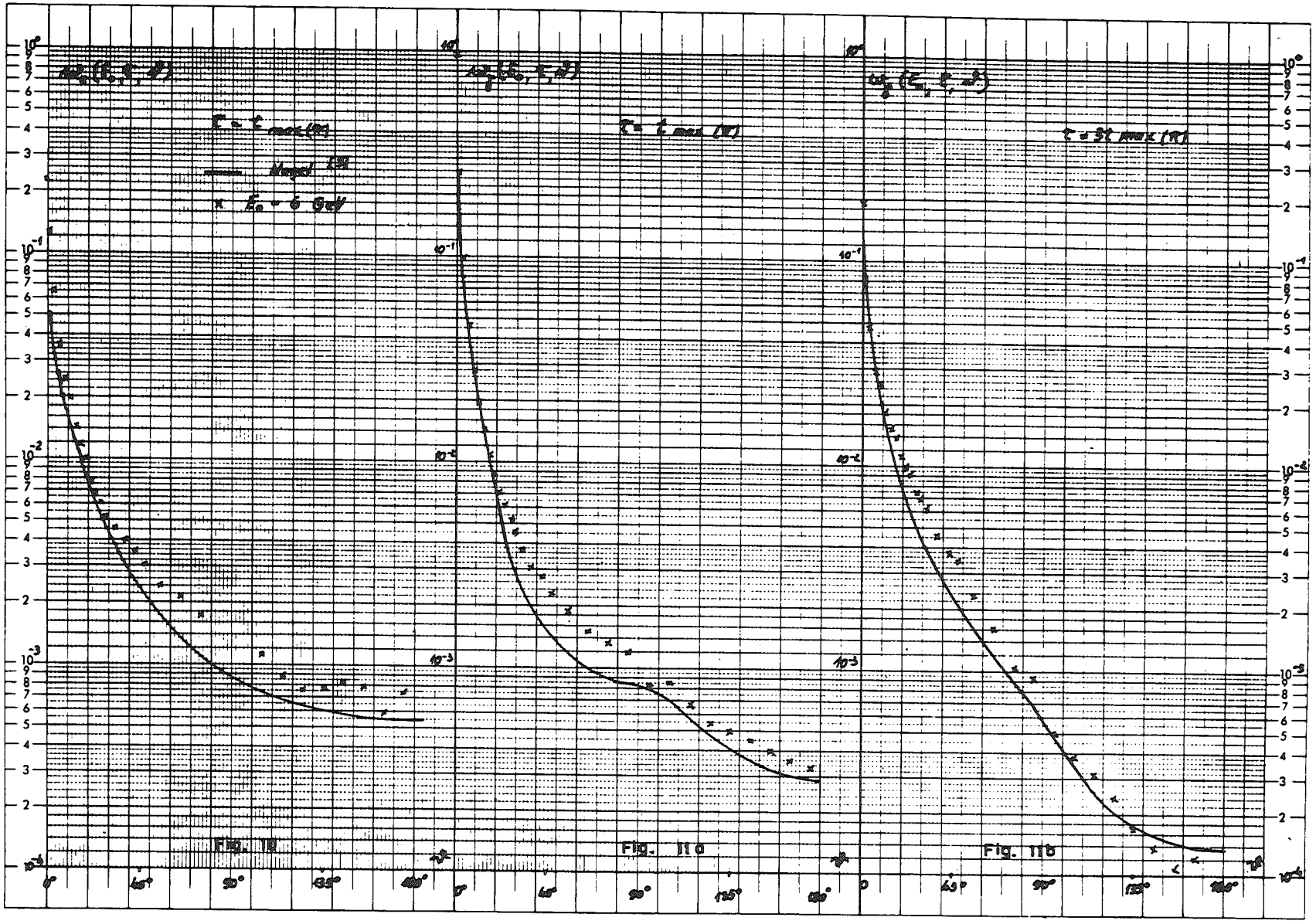

Fig. 10

Fig. 11 a

Fig. 11 b

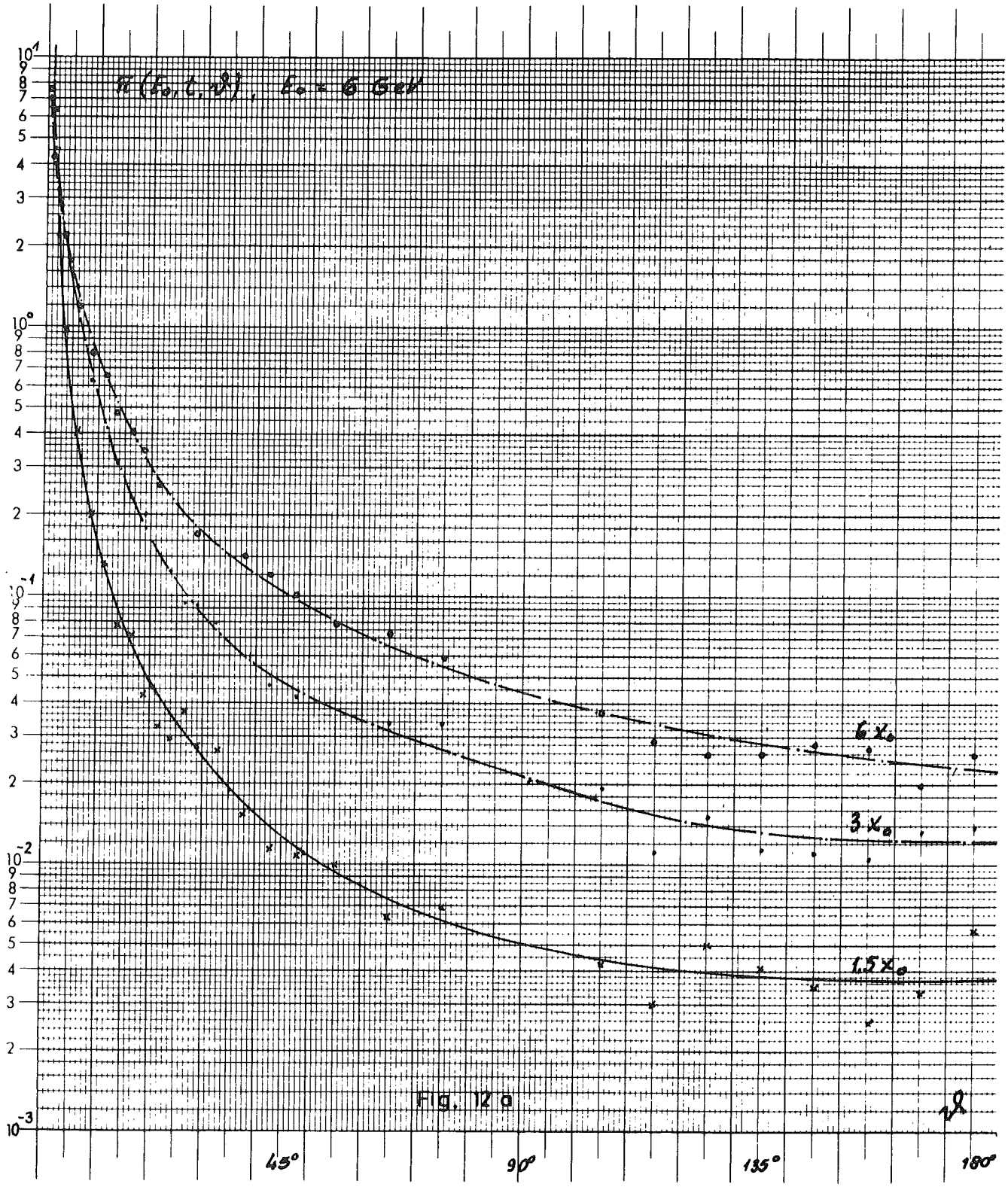

Fig. 12 a

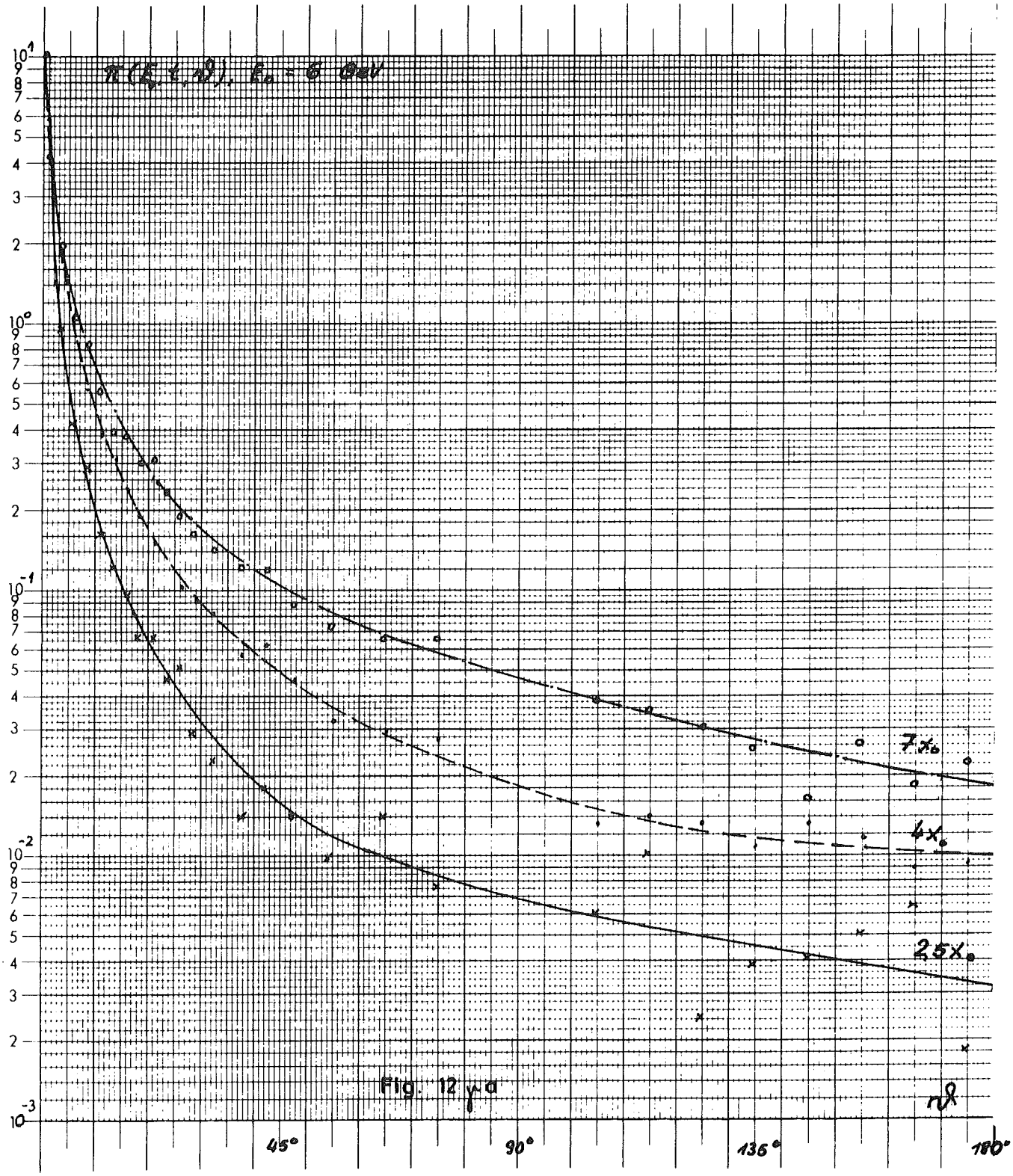

Fig. 12 γ-a

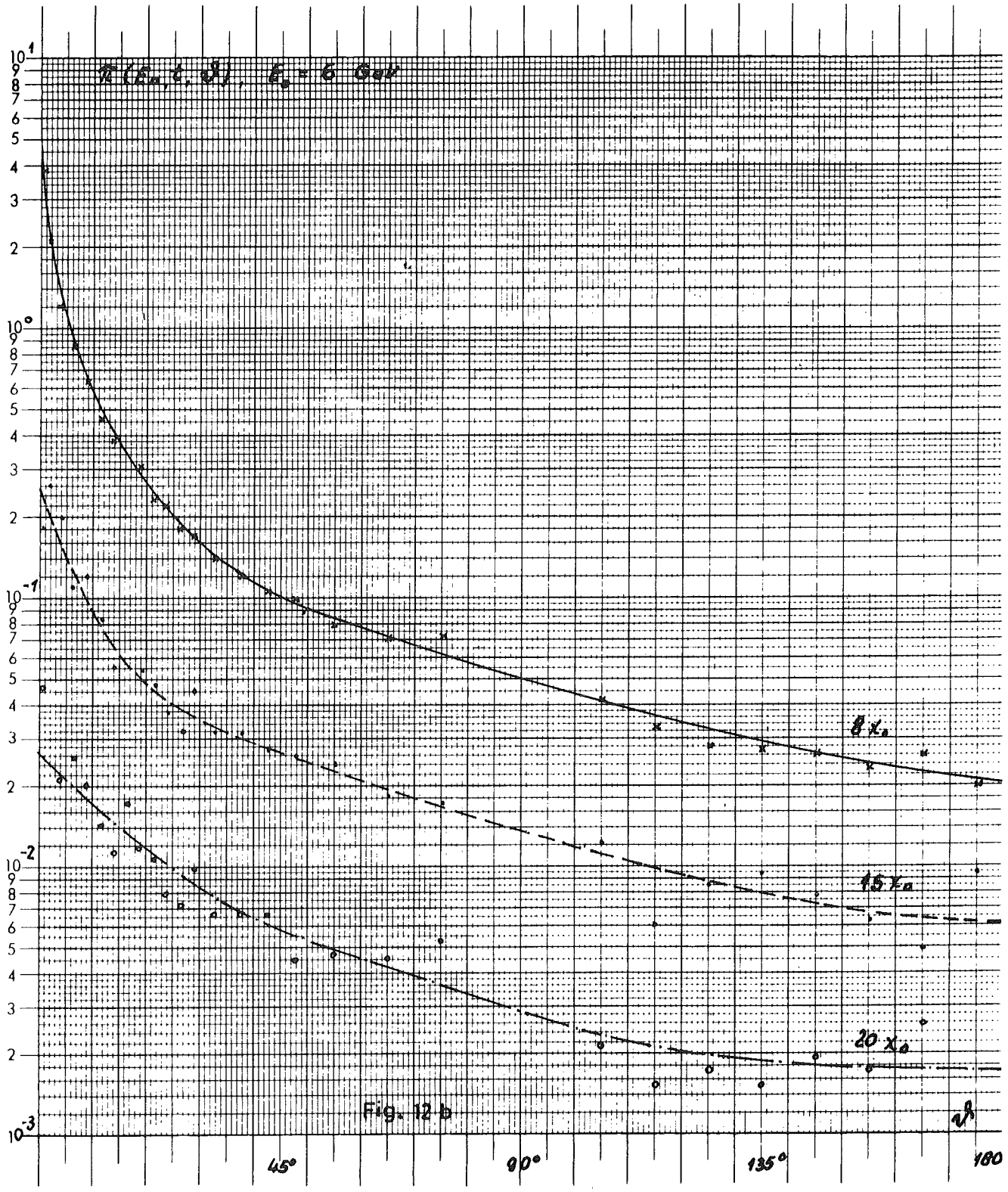
$\pi(E_a, t, \vartheta)$, $E_0 = 6$ GeV
10^{1}
10^{0}
10^{-1}
10^{-2}
10^{-3}
$8\,X_0$
$15\,X_0$
$20\,X_0$
45°
90°
135°
180
ϑ

Fig. 12 b

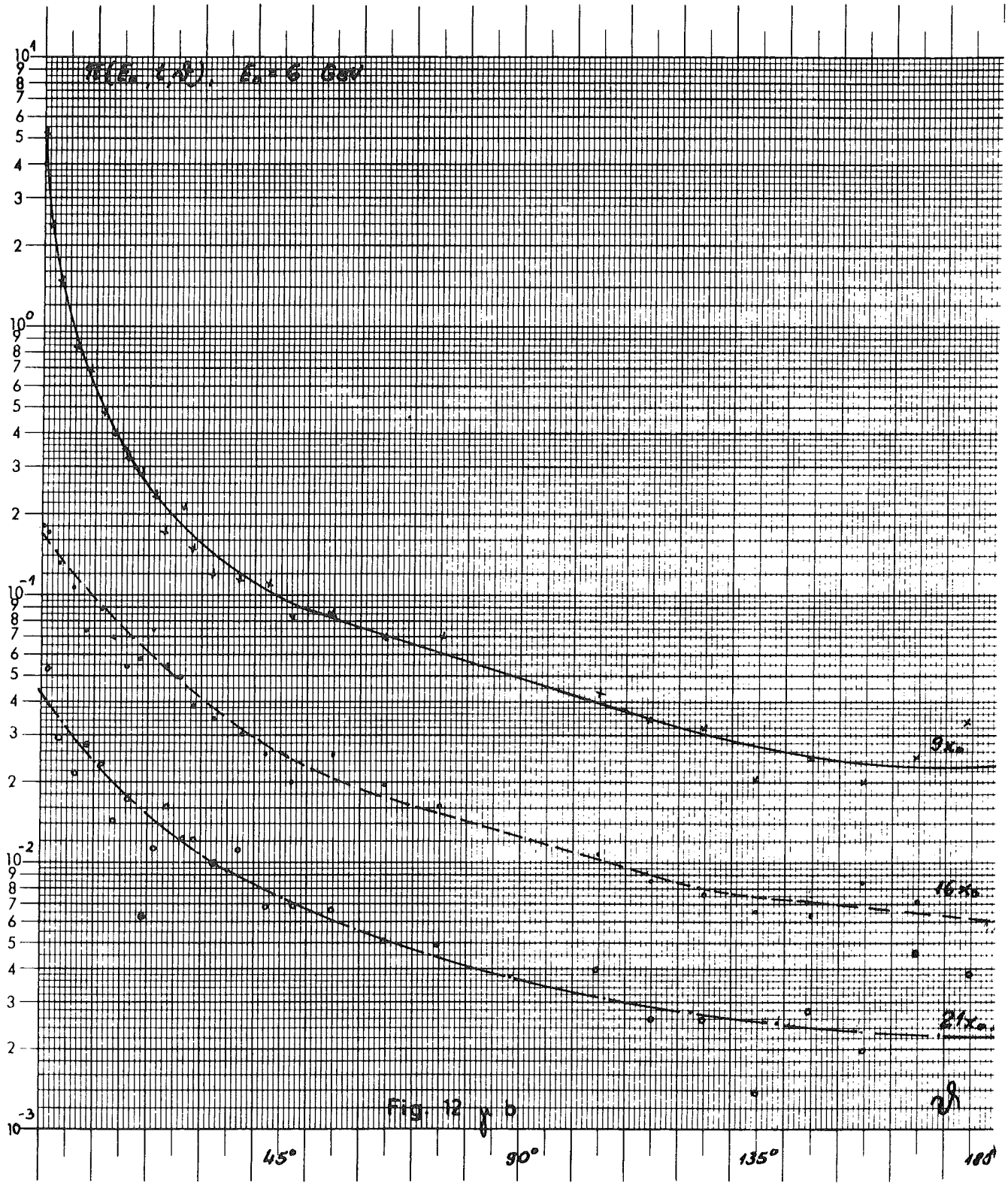
$\pi(E_\pi, \vartheta, \varphi)$, $E_\pi = 6$ GeV
10^1
10^0
10^{-1}
10^{-2}
10^{-3}
9 x_0
16 x_0
21 x_0
45°
90°
135°
180°
ϑ

Fig. 12 b

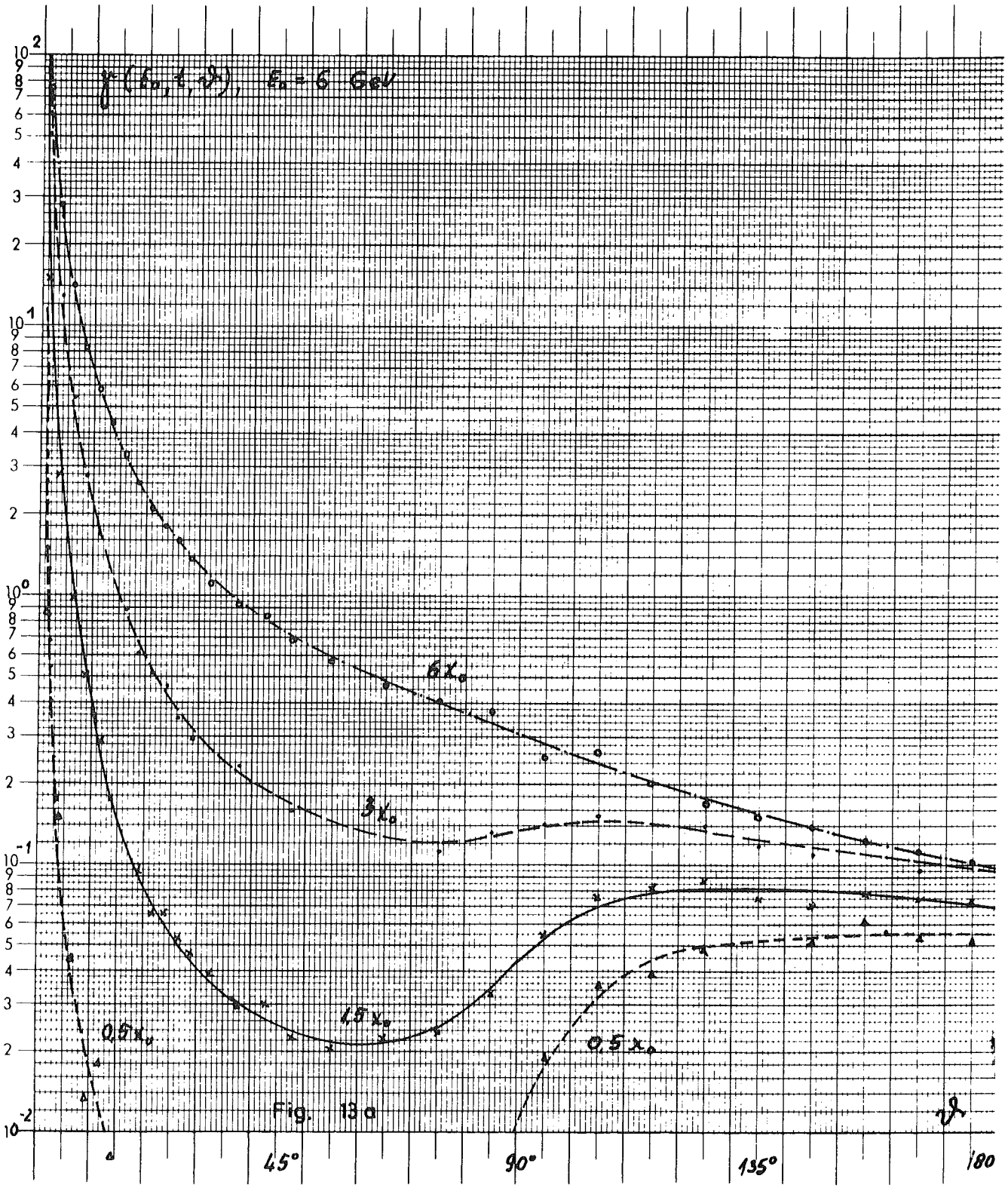
$j(E_0, t, \vartheta)$, $E_0 = 6$ GeV
$6 x_0$
$3 x_0$
$1.5 x_0$
$0.5 x_0$
$0.5 x_0$
45°
90°
135°
180
ϑ

Fig. 13 a

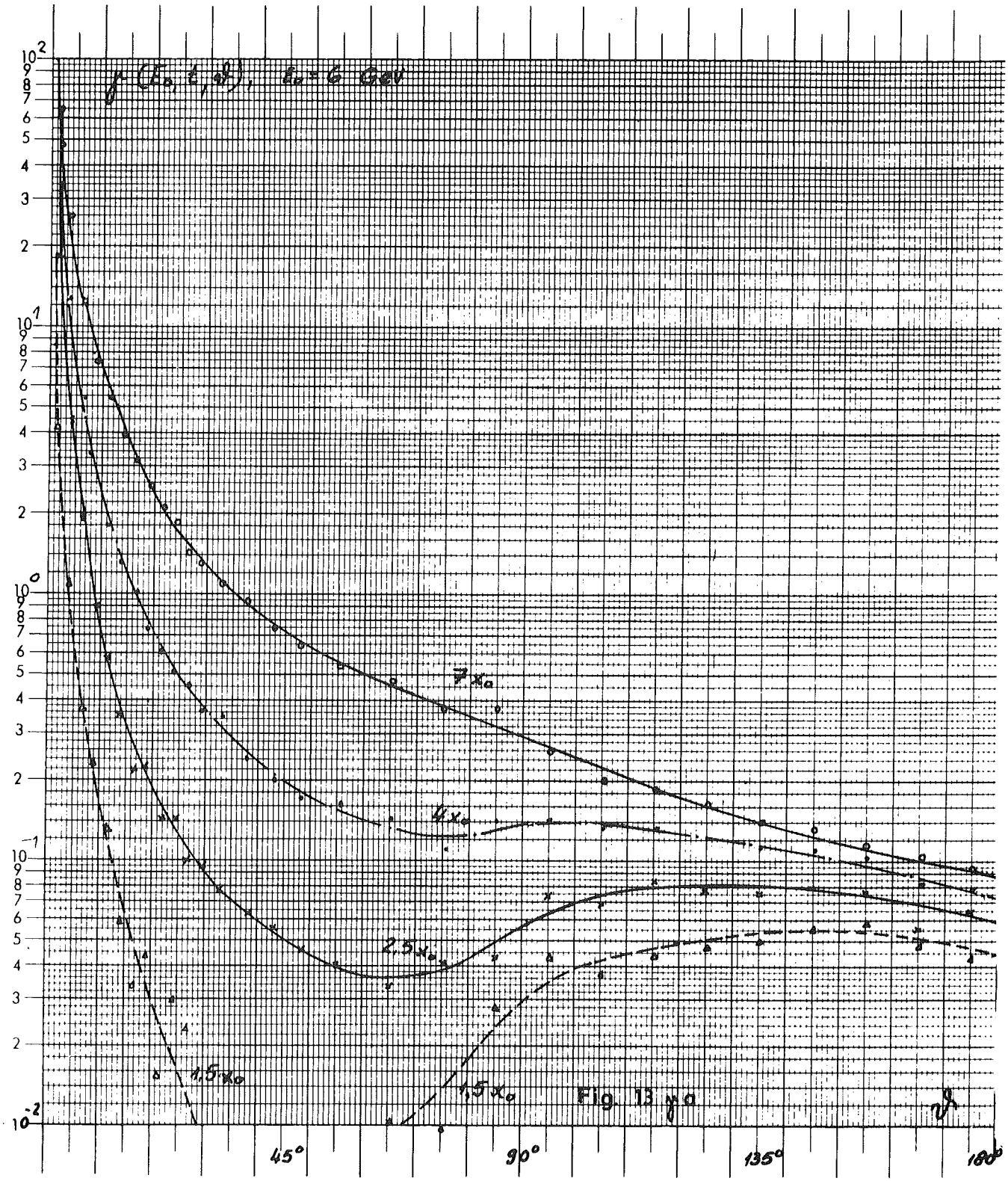

Fig. 13 γa

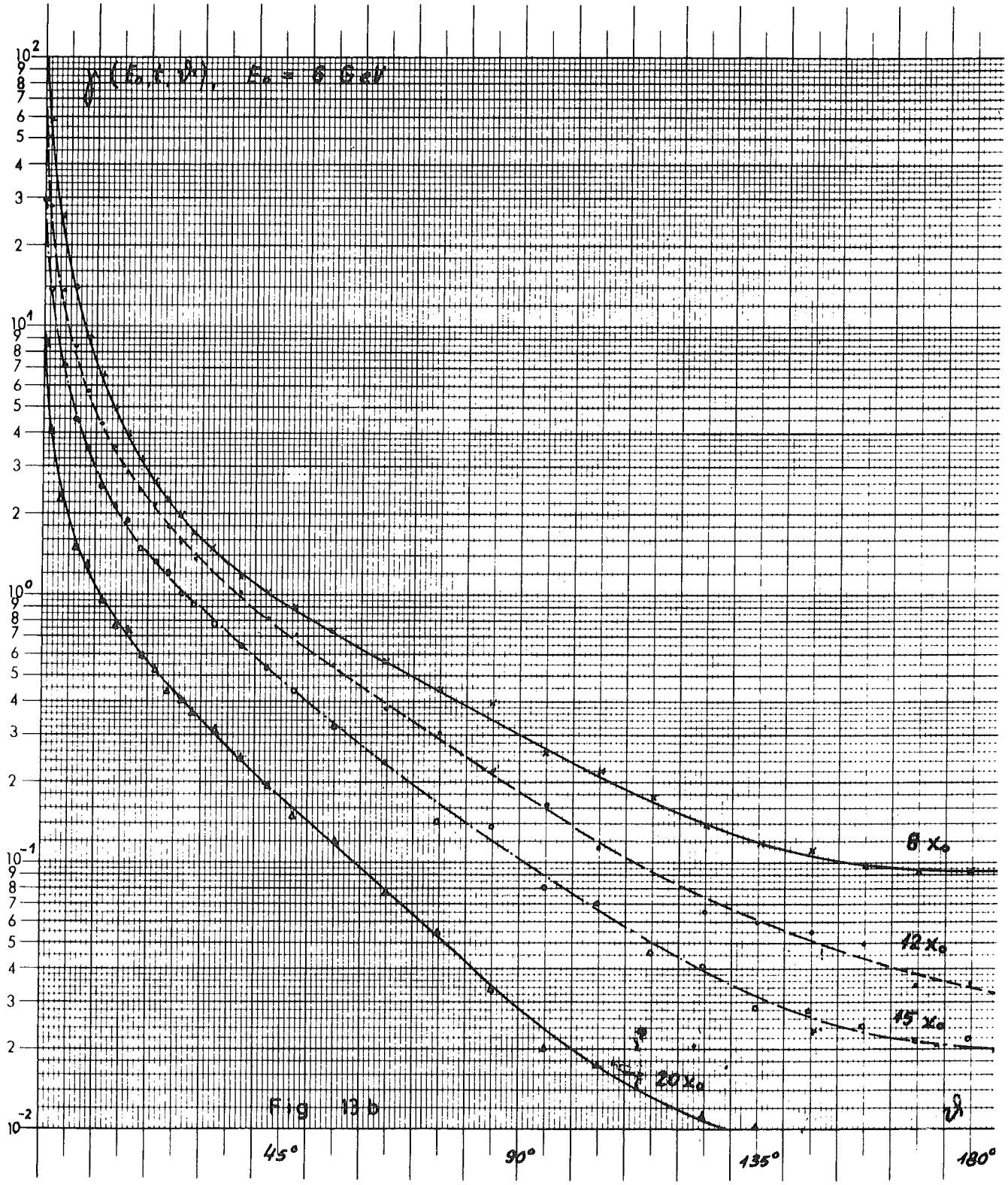
$\Phi(E_0, t, \vartheta)$, $E_0 = 6$ GeV
10^2
10^1
10^0
10^{-1}
10^{-2}
6 X_0
12 X_0
15 X_0
20 X_0
45°
90°
135°
180°
ϑ

Fig 13 b

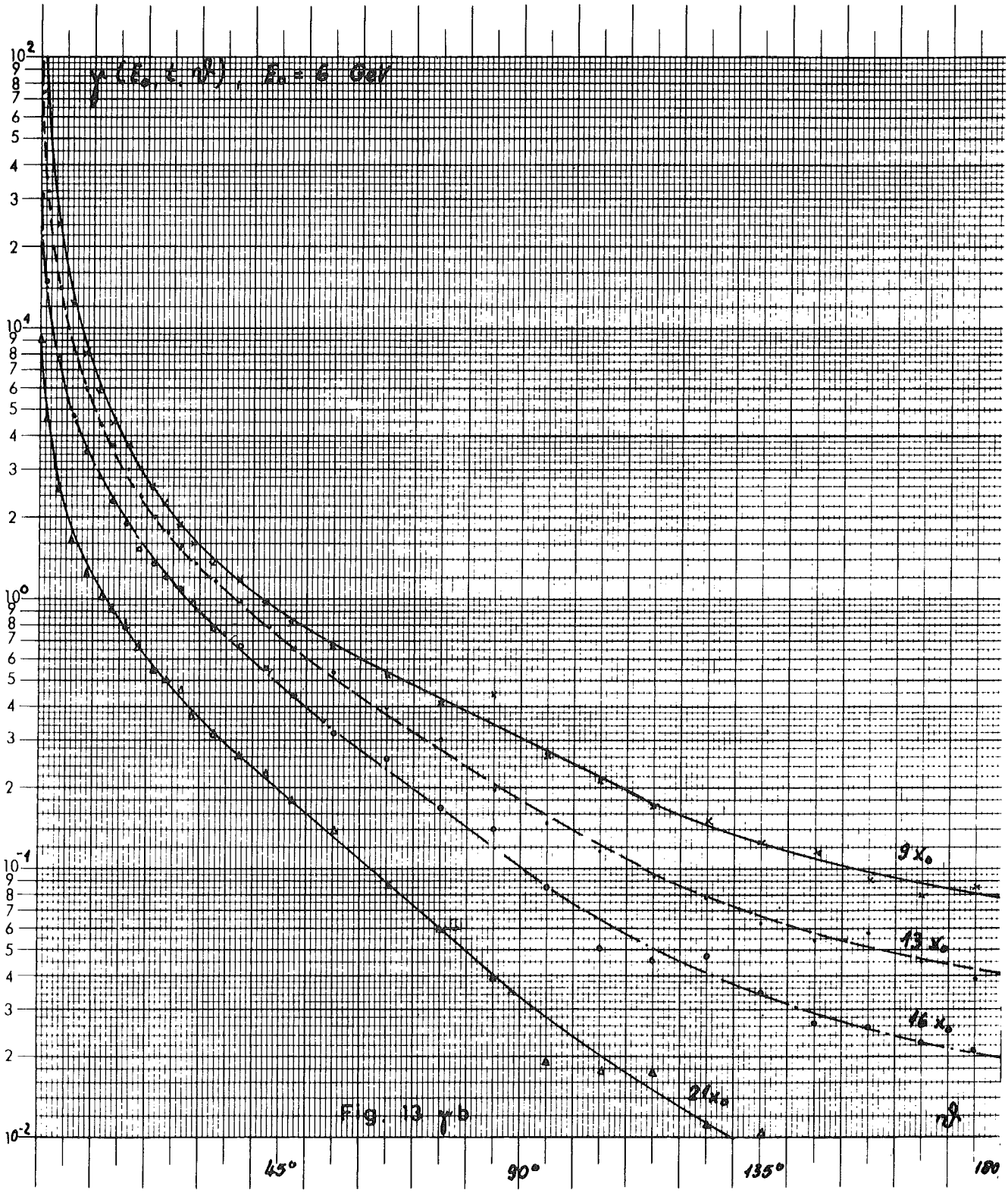

Fig. 13 γb

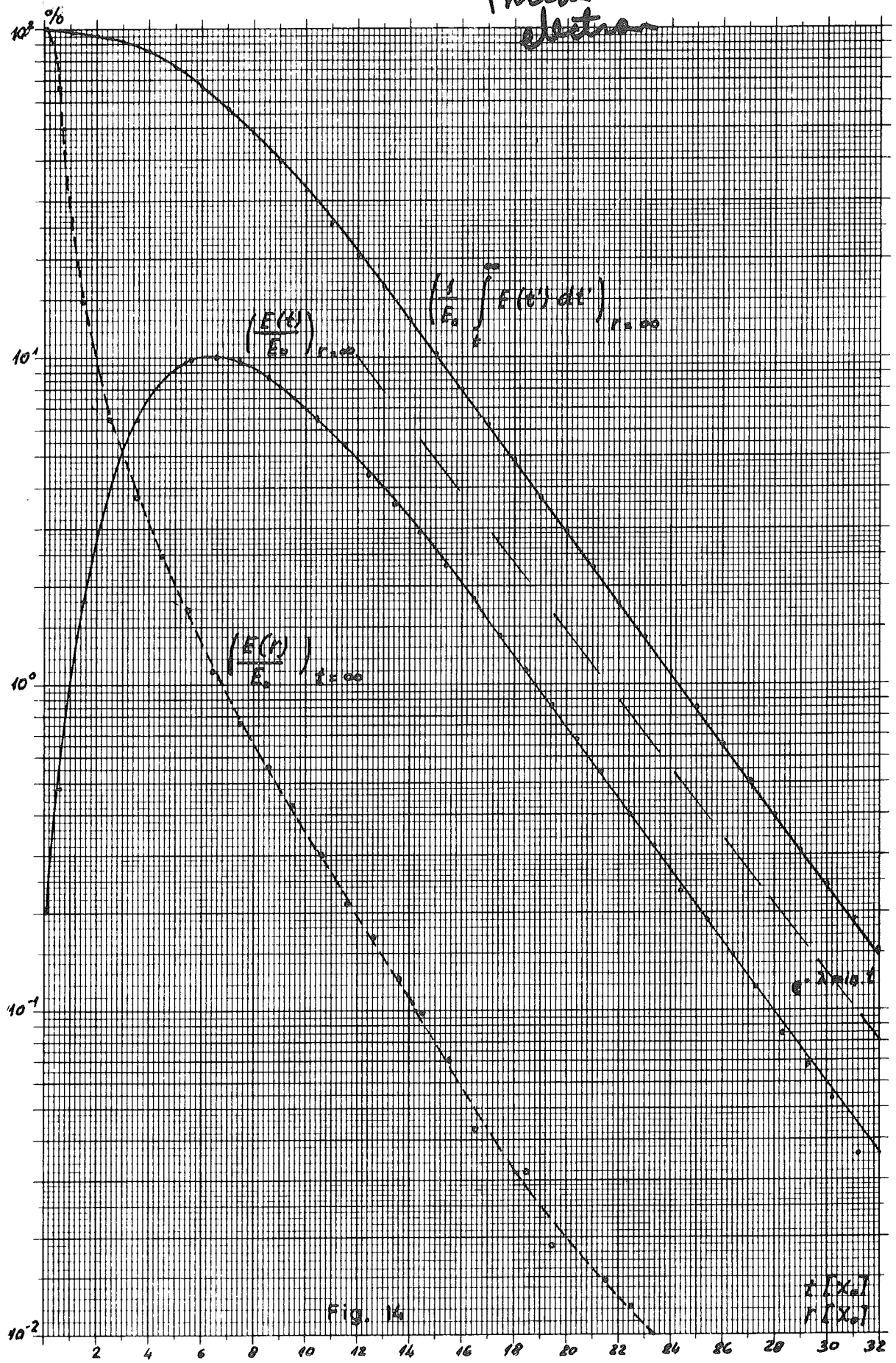
incident electron
%
10^2
10^1
10^0
10^{-1}
10^{-2}
$\left(\frac{E(t)}{E_0}\right)_{r=\infty}$
$\left(\frac{1}{E_0}\int_t^\infty E(t')\,dt'\right)_{r=\infty}$
$\left(\frac{E(t)}{E_0}\right)_{t=\infty}$
$e^{-\lambda=1.6\cdot t}$
$t\,[X_0]$
$r\,[X_0]$
2
4
6
8
10
12
14
16
18
20
22
24
26
28
30
32

Fig. 14

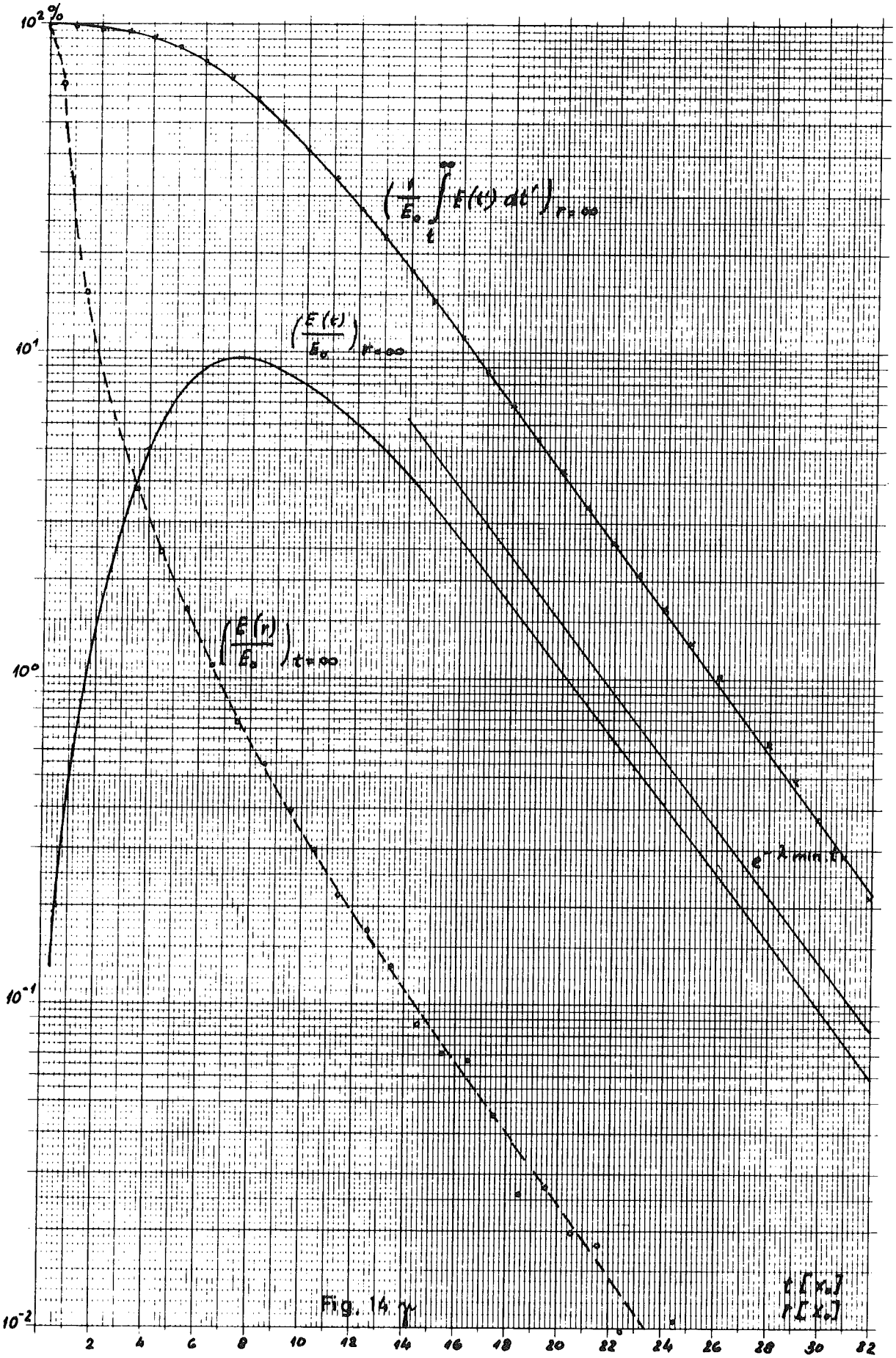
10^2 %
10^1
10^0
10^{-1}
10^{-2}
$\left(\frac{1}{E_0}\int_t^\infty E(t)\,dt'\right)_{r=\infty}$
$\left(\frac{E(t)}{E_0}\right)_{r=\infty}$
$\left(\frac{E(r)}{E_0}\right)_{t=\infty}$
$e^{-\lambda_{min.}t}$
2 4 6 8 10 12 14 16 18 20 22 24 26 28 30 32
t [χ_0]
r [χ_0]

Fig. 14

$\frac{\Delta E_0}{E_0} = \frac{1}{E_0}\int_0^t \int_1^\infty E(x',t')\,dx'dt'$ incident electro-

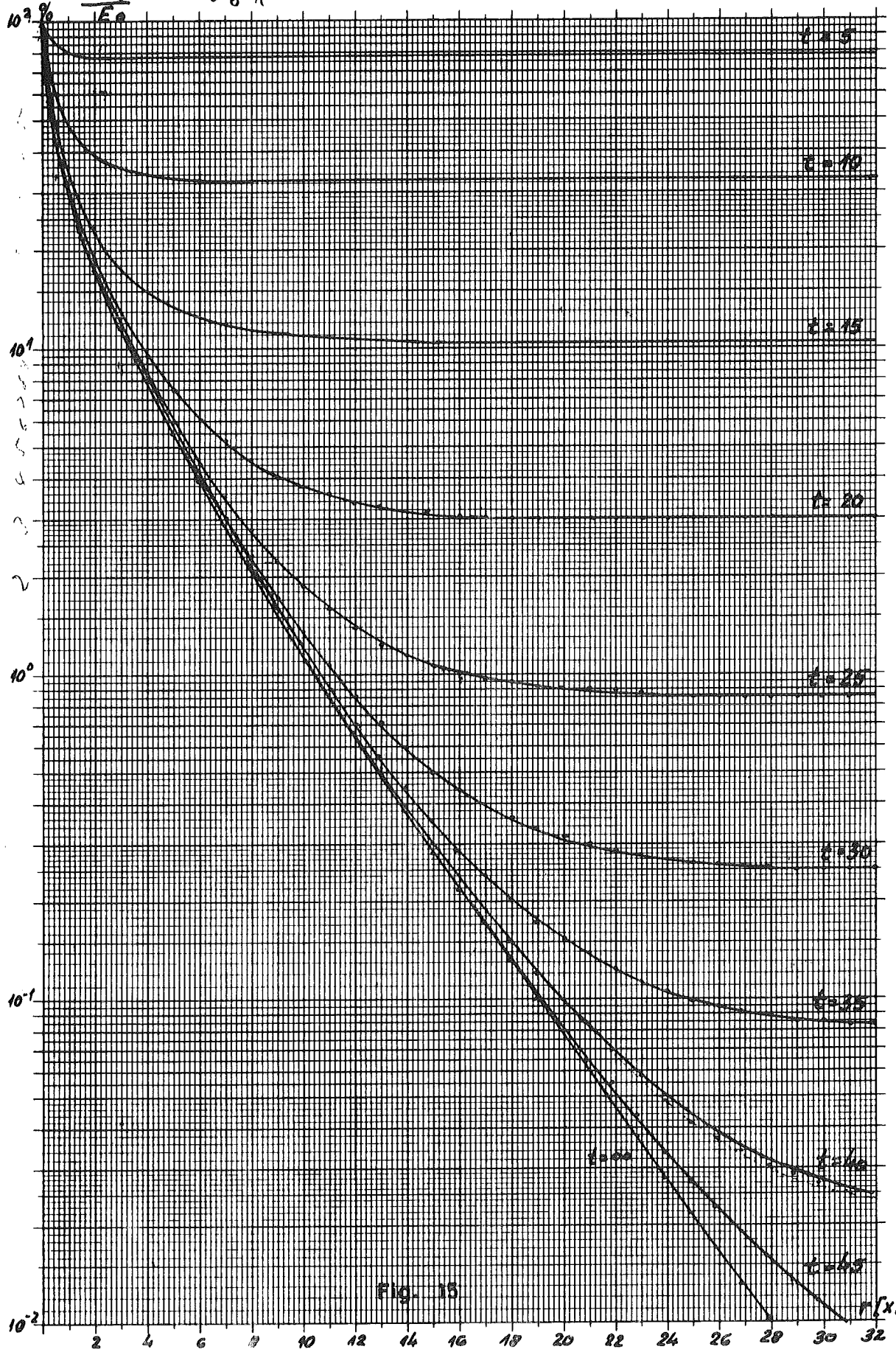

Fig. 15

incident photon

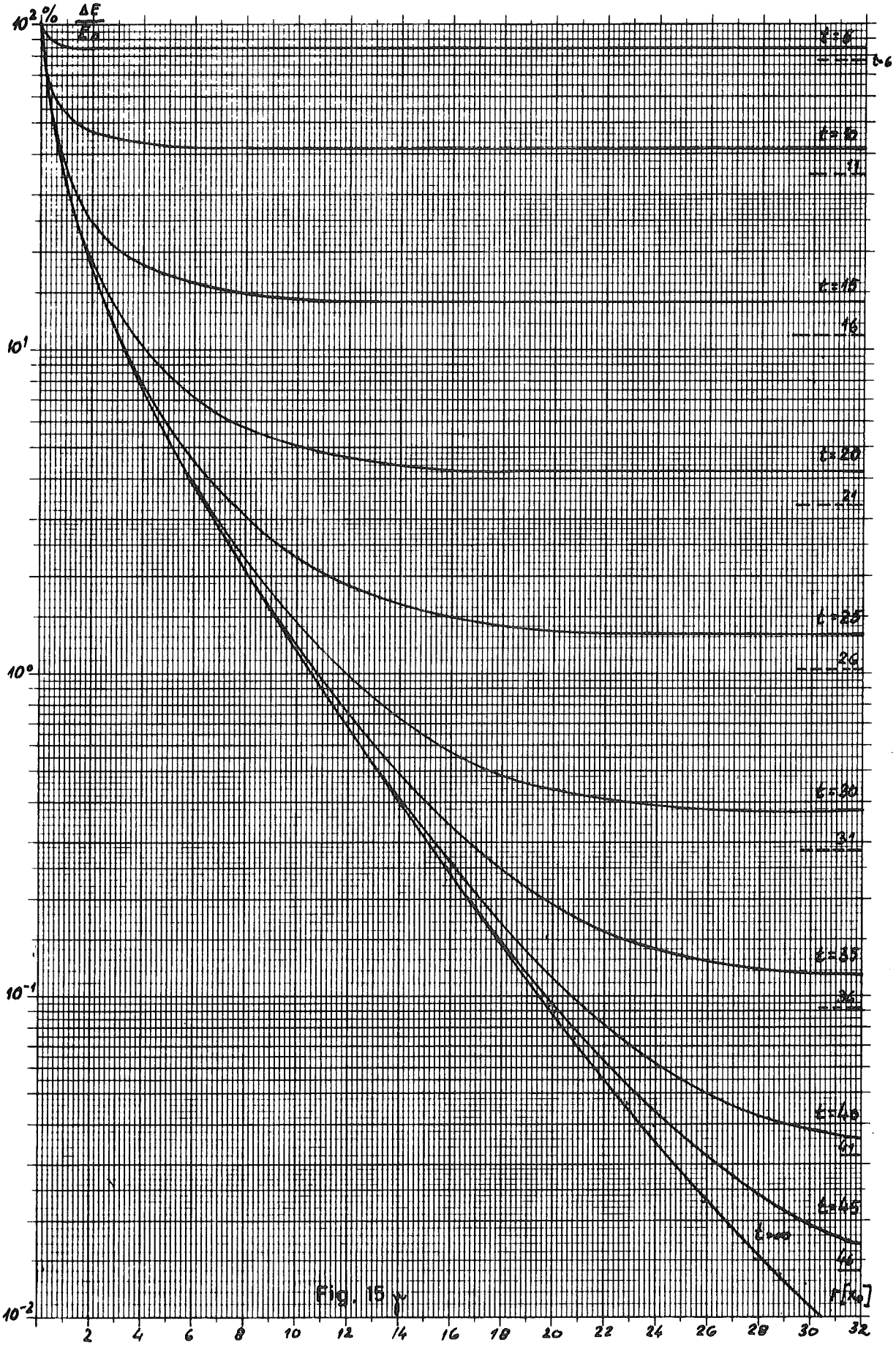

Fig. 15

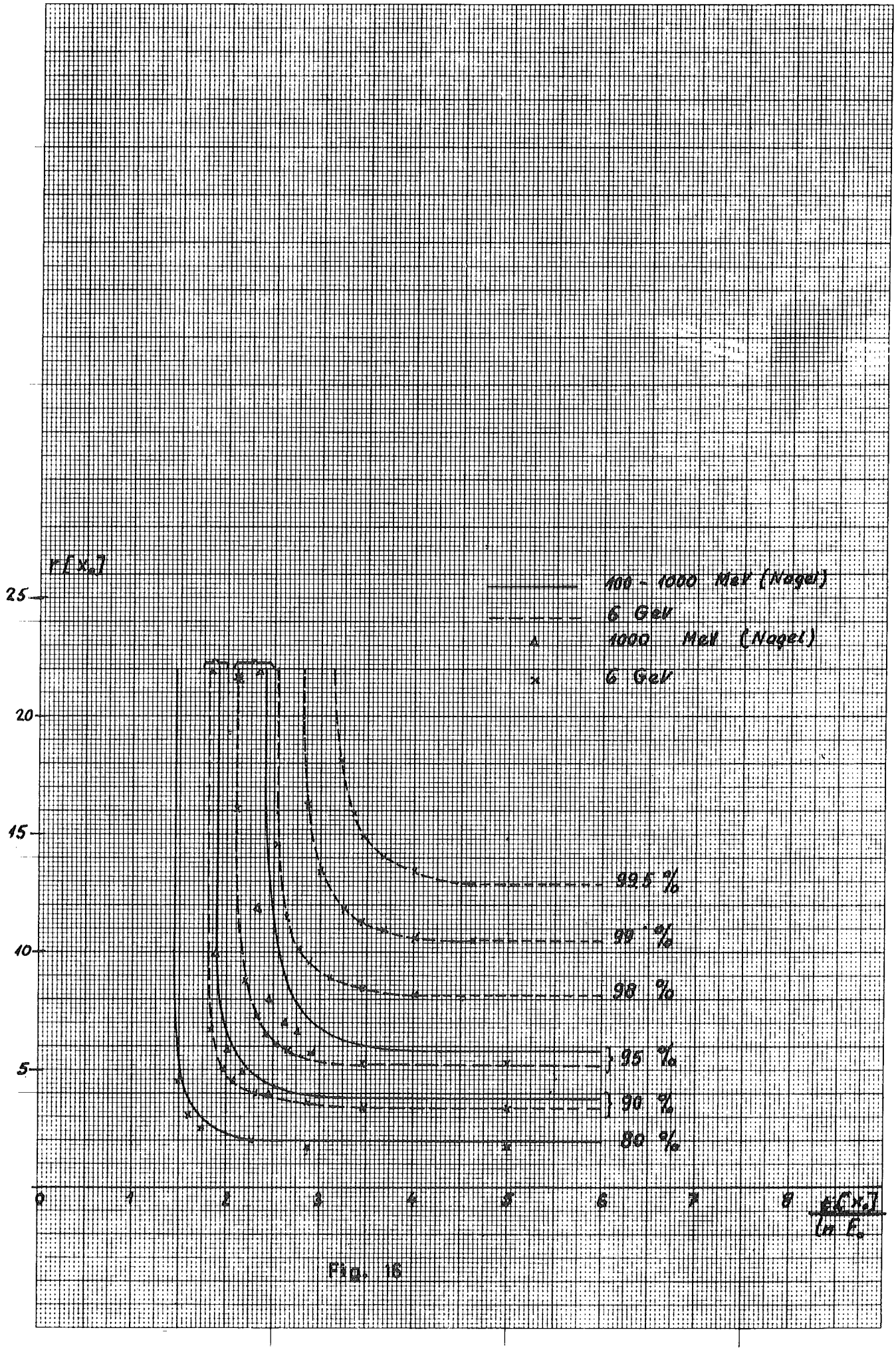
r[x₀]
25
20
15
10
5
0
1
2
3
4
5
6
7
8
100 - 1000 Mev (Nagel)
6 Gev
1000 Mev (Nagel)
6 Gev
99,5 %
99 %
98 %
95 %
90 %
80 %
E[x₀] / E₀

Fig. 16